Received: 13 July 2022 | Revised: 16 September 2022 | Accepted: 25 September 2022

DOI: 10.1002/hipo.23474

REVIEW

WILEY

Methods to study adult hippocampal neurogenesis in humans and across the phylogeny

Julia Terreros-Roncal[1,2,3] | Miguel Flor-García[1,2,3] | Elena P. Moreno-Jiménez[1,2,3] | Carla B. Rodríguez-Moreno[1,3] | Berenice Márquez-Valadez[1,3] | Marta Gallardo-Caballero[1,2,3] | Alberto Rábano[4] | María Llorens-Martín[1,3]

[1]Department of Molecular Neuropathology, Centro de Biología Molecular "Severo Ochoa" (CBMSO), Spanish Research Council (CSIC)—Universidad Autónoma de Madrid (UAM), Madrid, Spain

[2]Department of Molecular Biology, Faculty of Sciences, Universidad Autónoma de Madrid, Madrid, Spain

[3]Center for Networked Biomedical Research on Neurodegenerative Diseases (CIBERNED), Madrid, Spain

[4]Neuropathology Department, CIEN Foundation, Madrid, Spain

Correspondence
María Llorens-Martín, Department of Molecular Neuropathology, Centro de Biología Molecular "Severo Ochoa" (CBMSO), Spanish Research Council (CSIC)—Universidad Autónoma de Madrid (UAM), Madrid, Spain.
Email: m.llorens@csic.es

Funding information
Association for Frontotemporal Degeneration; Banco de Santander; Center for Networked Biomedical Research on Neurodegenerative Diseases; Consejo Nacional de Ciencia y Tecnología (CONACYT), Grant/Award Number: 385084; European Research Council, Grant/Award Number: ERC-CoG-2020-101001916; Fundación Ramón Areces; Secretaria de Educación, Ciencia Tecnología e Innovación (SECTEI) of the Regional Government of Ciudad de México (CDMX), Grant/Award Number: SECTEI/159/2021; Spanish Ministry of Economy and Competitiveness, Grant/Award Numbers: PID2020-113007RB-I00, RYC-2015-171899,

Abstract

The hippocampus hosts the continuous addition of new neurons throughout life—a phenomenon named adult hippocampal neurogenesis (AHN). Here we revisit the occurrence of AHN in more than 110 mammalian species, including humans, and discuss the further validation of these data by single-cell RNAseq and other alternative techniques. In this regard, our recent studies have addressed the long-standing controversy in the field, namely whether cells positive for AHN markers are present in the adult human dentate gyrus (DG). Here we review how we developed a tightly controlled methodology, based on the use of high-quality brain samples (characterized by short postmortem delays and ≤24 h of fixation in freshly prepared 4% paraformaldehyde), to address human AHN. We review that the detection of AHN markers in samples fixed for 24 h required mild antigen retrieval and chemical elimination of autofluorescence. However, these steps were not necessary for samples subjected to shorter fixation periods. Moreover, the detection of labile epitopes (such as Nestin) in the human hippocampus required the use of mild detergents. The application of this strictly controlled methodology allowed reconstruction of the entire AHN process, thus revealing the presence of neural stem cells, proliferative progenitors, neuroblasts, and immature neurons at distinct stages of differentiation in the human DG. The data reviewed here demonstrate that methodology is of utmost importance when studying AHN by means of distinct techniques across the phylogenetic scale. In this regard, we summarize the major findings made by our group that emphasize that overlooking fundamental technical principles might have consequences for any given research field.

Julia Terreros-Roncal, Miguel Flor-García, and Elena P. Moreno-Jiménez contributed equally as co-first authors.

SAF-2017-82185-R; The Alzheimer's Association, Grant/Award Numbers: 2015-NIRG-340709, AARG-17-528125, AARG-17-528125-RAPID

KEYWORDS
adult hippocampal neurogenesis, antigen retrieval, autofluorescence, human, immunohistochemistry

1 | INTRODUCTION

Adult hippocampal neurogenesis (AHN) encompasses the functional integration of new dentate granule cells (DGCs) into the hippocampal trisynaptic circuit throughout life (Zhao et al., 2006). The continuous addition of new neurons confers the adult brain with an extraordinary reserve of plasticity. Indeed, AHN participates in hippocampal-dependent learning (Sahay et al., 2011; Shors et al., 2001) and mood regulation (Hill et al., 2015), and it has been proposed to play a role in memory loss (Akers et al., 2014). The occurrence of AHN is widespread among the >120 mammalian species in which it has been assessed (see Table 1 for a complete list), including rodents (Altman, 1963), shrews (Gould et al., 1997), sheep (Brus et al., 2013), bats (Chawana et al., 2014, 2016, 2020; Gatome et al., 2010), elephants (Patzke, Olaleye, et al., 2014), non-human primates (Franjic et al., 2022; Gould et al., 1999; Hao et al., 2022; Kohler et al., 2011), and humans (Boldrini et al., 2018; Eriksson et al., 1998; Flor-Garcia et al., 2020; Knoth et al., 2010; Manganas et al., 2007; Moreno-Jimenez et al., 2019, 2021; Spalding et al., 2013; Terreros-Roncal et al., 2021). There may be a few exceptions: two studies did not find evidence of AHN in northern minke whales or in harbor porpoises (Patzke et al., 2015), nor in a small number of echolocating microbats captured from the wild (Amrein et al., 2007). However, these results lack further replication to date. Although AHN has been extensively characterized in rodents, technical and ethical aspects may have limited the pace of discoveries in the human AHN field. In this regard, although a few studies failed to detect markers of neurogenesis in the adult human hippocampus (Dennis et al., 2016; Franjic et al., 2022; Sorrells et al., 2018), most literature available supports the occurrence of AHN in our species (Boldrini et al., 2018; Eriksson et al., 1998; Knoth et al., 2010; Moreno-Jimenez et al., 2019; Spalding et al., 2013; Terreros-Roncal et al., 2021; Tobin et al., 2019; W. Wang et al., 2022) (see Table 2 for an extended list). This review addresses the technical considerations that, in our view, lie behind most controversial aspects and ambiguities related to AHN studies in humans (Flor-Garcia et al., 2020; Moreno-Jimenez et al., 2021).

AHN has various sequential stages (Figure 1) (Kempermann et al., 2004). Two main strategies, namely the birthdating of newly generated proliferative cells (Altman, 1963) and the detection of specific cell markers (Kempermann et al., 2004), have been used to thoroughly characterize AHN. This process relies on the presence of radial glia-like (RGL) neural stem cells (NSCs) in the dentate gyrus (DG) germinative matrix, namely the subgranular zone (SGZ). NSCs give rise to transit-amplifying progenitors and neuroblasts, which show a high proliferative capacity and expand neurogenic cell populations while progressively becoming committed to the neuronal lineage. In contrast, NSCs are mostly quiescent, a phenomenon proposed to be accentuated in aged individuals to preserve the pluripotency of these cells throughout life (Bottes et al., 2021; Harris et al., 2021). Neuroblasts are characterized by an immature neuronal morphology and the expression of proteins related to the cytoskeleton and cell plasticity, such as doublecortin (DCX) and polysialylated-neural cell adhesion molecule (PSA-NCAM). After exiting the cell cycle, newborn neurons go through sequential differentiation stages before becoming fully mature. Throughout their maturation, DGCs progressively occupy deeper positions in the granule cell layer (GCL) and show not only more complex dendritic morphologies but also the presence of functional dendritic spines and axons (Zhao et al., 2006).

2 | THE HISTORY OF HUMAN ADULT HIPPOCAMPAL NEUROGENESIS

As in the rodent AHN field (Altman, 1963), birthdating strategies were initially used to assess the occurrence of AHN in humans. In 1998, Eriksson et al. observed that the peripheral administration of 5-bromo-2′-deoxyuridine (BrdU) results in the uptake of this molecule into discrete proliferative cells of the human DG, thereby supporting the occurrence of AHN in our species (Eriksson et al., 1998). That pioneering study showed that, several weeks/months after BrdU administration, BrdU-labeled cells express neuronal markers. In 2014, Eriksson's results were further confirmed by Ernst et al. (2014), who used a different thymidine analog (5-iodo-2′-deoxyuridine, IdU) and also observed the incorporation of this molecule into the adult human DG. Their results were further corroborated by a novel methodology, developed by Frisen's group, to measure the incorporation of C^{14} into the brain (Spalding et al., 2013). Their studies determined that ~700 new neurons per hemisphere are added daily to the human DG.

In recent decades, numerous studies have used immunohistochemistry (IHC) to assess the occurrence of AHN in the human brain. Most of this work (see Table 2) systematically reported the presence of cells positive for AHN markers throughout human life (Boldrini et al., 2018; Cipriani et al., 2018; Eriksson et al., 1998; Knoth et al., 2010; Moreno-Jimenez et al., 2019; Spalding et al., 2013; Terreros-Roncal et al., 2021). In this regard, despite decreasing throughout physiological aging, AHN remains detectable until the ninth decade of life (Boldrini et al., 2009; Knoth et al., 2010; Moreno-Jimenez et al., 2019; Terreros-Roncal et al., 2021). Paradoxically, other studies failed to detect cells positive for such markers in the same region (Sorrells et al., 2018), although some of the authors of the aforementioned publication affirmed the existence of human AHN in previous studies (Galan et al., 2017). Given the specific conditions required to perform and validate IHC results on human tissue (Boekhoorn et al., 2006; Flor-Garcia et al., 2020), technical aspects need, more than ever, to be carefully dissected and taken into consideration when addressing these seemingly contradictory results.

TABLE 1 List of studies addressing the occurrence of adult hippocampal neurogenesis (AHN) in distinct mammalian species

Infraclass	Order	Species	Reference	Conclusions
Marsupialia	**Dasyuromorphia**	**Fat-tailed dunnart** (*Sminthopsis crassicaudata*)	(Harman et al., 2003)	The occurrence of AHN was demonstrated using thymidine-H^3. Stress and age reduced the number of newly generated DGCs.
		Tasmanian devil (*Sarcophilus harrisii*)	(Patzke et al., 2015)	Presence of DCX^+ immature neurons in the SGZ and GCL.
	Didelmorphia	**Opossum** (*Monodelphis domestica*)	(Grabiec et al., 2009)	Lifetime occurrence of AHN, despite a reduction with age. Buspirone boosted proliferation in the DG of adult and aged opossums.
Placental mammals	**Eulipotyphla**	**Hedgehog** (*Erinaceus concolor*), **Mole** (*Talpa europaea*)	(Bartkowska et al., 2010)	Presence of DCX^+ and Ki-67^+ cells in the SGZ and GCL. No colocalization between DCX and glial markers such as vimentin or GFAP.
		Common shrew (*Sorex araneus*), **Pygmy shrew** (*Sorex minutus*)	(Bartkowska et al., 2008)	No $BrdU^+$ cells were detected in the DG from spring to autumn.
	Lagomorpha	**New Zealand White** (*Oryctolagus cuniculus*)	(Zhu et al., 2003)	Presence of RNR^+ proliferative cells in the SGZ. Morphological characterization of RNR^+ cells, which did not express markers of differentiated neurons or glial cells, except a fraction that co-expressed GFAP.
	Rodentia	**Degus** (*Octodon degus*)	(Kumazawa-Manita et al., 2013)	$BrdU^+$ and PSA-$NCAM^+$ cells were found in the DG. T-shape rake learning increases AHN and the proportion of new synapses formed in the CA3 field.
		African giant rat (*Cricentomys gambianus*)	(Olude et al., 2014)	Presence of DCX^+ and Ki-67^+ cells in the DG. Adults presented lower cell numbers than juveniles.
		Gray squirrels (*Sciurus carolinensis*)	(Lavenex et al., 2000)	BrdU incorporation in the DG. No seasonal differences in cell proliferation rate or in total neuron number were observed.
			(Barker et al., 2005)	Gray squirrels showed three times the density of Ki-67^+ proliferating cells in the DG than chipmunks, which have simple food storage strategies. Both species showed similar density of immature DCX^+ neurons. The number of Ki-67^+ proliferative cells in gray squirrels and the density of DCX^+ immature neurons in chipmunks decreased with age.
		Yellow-pine chipmunks (*Neotamias amoenus*)	(Barker et al., 2005)	Gray squirrels showed three times the density of Ki-67^+ proliferating cells in the DG than chipmunks, which have simple food storage strategies. Both species showed similar density of immature DCX^+ neurons. The number of Ki-67^+ proliferative cells in gray squirrels and the density of DCX^+ immature neurons in chipmunks decreased with age.
		Red squirrel (*Tamiasciurus hudsonicus*)	(Johnson et al., 2010)	Presence of Ki-67^+ proliferative cells and DCX^+ immature neurons in the DG. Two populations of animals with distinct food-storage strategies showed similar cell densities and age-dependent decline.
		Cape mole-rats (*Georychus capensis*), **Highveld mole-rats** (*Cryptomys hottentotus pretoriae*)	(Amrein et al., 2014)	Ki-67^+ proliferative cells, DCX^+ or PSA-$NCAM^+$ immature neurons, and DGCs were found in low numbers of all the species. Proliferation was regulated independently of life expectancy and habitat. Neuronal differentiation reflected species-specific demands, which were lower in subterranean rodents.

(Continues)

TABLE 1 (Continued)

Infraclass	Order	Species	Reference	Conclusions
		Naked mole-rats (*Heterocephalus glaber*)	(Amrein et al., 2014)	Ki-67$^+$ proliferative cells, DCX$^+$ or PSA-NCAM$^+$ immature neurons, and DGCs were found in low numbers of all the species. Proliferation was regulated independently of life expectancy and habitat. Neuronal differentiation reflected species-specific demands, which were lower in subterranean rodents.
			(Peragine et al., 2014)	AHN was present in naked mole-rats. Compared to subordinates, dominant breeders have reduced numbers of DCX$^+$ immature neurons in the DG. Higher number of DCX$^+$ immature neurons in opposite-sex- than in same-sex-paired subordinates. No influence of gonadal steroids and DCX immunoreactivity.
		Guinea pig (*Cavia porcellus*)	(Islam et al., 2003)	Presence of PSA-NCAM$^+$ and NOS$^+$ cells in the GCL.
			(Wan et al., 2019)	BrdU$^+$ cells positive for Ki67, Sp8, and DCX in the adult SGZ. These cell populations peaked at the late gestational stages in comparison to non-pregnant females.
			(Wan et al., 2021)	Presence of Ki-67$^+$and DCX$^+$ cells in the DG. Radiation causes loss of DCX$^+$ cells in the SGZ and reduction in the number of Ki-67$^+$ proliferative cells and in the DCX$^+$ immature neurons of the dorsal hippocampus.
		Meadow vole (*Microtus pennsylvanicus*)	(Galea et al., 1999)	Incorporation of thymidine-H^3 in the DG. Higher proliferation rate in females captured during the non-breeding season than those captured during the breeding season.
			(Ormerod et al., 2001)	Incorporation of thymidine-H^3 and BrdU in the DG. Higher density of proliferative cells in the GCL and the hilus in reproductively inactive females compared to active females. This density correlated negatively with serum estradiol levels. Higher rates of cell survival in the GCL and the hilus in reproductively active females.
		Prairie vole (*Microtus ochrogaster*)	(Fowler et al., 2002)	BrdU incorporation in the DG of females.
		Yellow necked wood mouse (*Apodemus flavicollis*) **Long-tailed wood mouse** (*Apodemus sylvaticus*) **Bank vole** (*Myodes glareolus*) **Pine vole** (*Microtus duodecimcostatus*)	(Amrein et al., 2004)	AHN was demonstrated in the 4 species, which showed distinct onset of age-driven decrease in AHN.
		Common mouse (*Mus musculus*)	(Kaplan et al., 1984)	Ultrastructural identification of thymidine-H^3-labeled mitotic neuronal precursors in the GCL of rats and mice.
			(Hochgerner et al., 2018)	Profiling of 5454 cells from the mouse hippocampus using sc-RNA seq. Reconstruction of the whole AHN trajectory from RGL cells to mature DGCs.
		Common rat (Rattus norvegicus)	(Altman, 1963)	Identification of a proliferative region in the adult rat DG.
			(Zhu et al., 2003)	Morphological characterization of RNR$^+$ proliferative cells, which do not express markers of differentiated neurons or glial cells, except a fraction that co-expressed GFAP. Colocalization between BrdU and RNR in proliferative cells.
			(McDonald et al., 2005)	Characterization of neuronal differentiation, maturation, and migration in the adult rat DG by means of BrdU incorporation, and DCX and CB expression. Reduction of cell generation with age.

TABLE 1 (Continued)

Infraclass	Order	Species	Reference	Conclusions
		Norway rat (Rattus norvegicus)	(Epp et al., 2009)	Presence of Ki-67$^+$ proliferative cells and DCX$^+$ immature neurons in the DG of both wild and bred rats. Higher numbers of Ki-67$^+$ and DCX$^+$ cells in juvenile wild rats than some bred rats, but no differences were observed with age in the former.
		Gerbils (*Meriones unguiculatus*)	(Dawirs et al., 1998)	BrdU incorporation. Haloperidol increased DGC proliferation.
			(Dawirs et al., 2000)	Presence of BrdU$^+$ proliferative cells in the DG throughout adult life and aging, despite a decline during juvenile life.
		Namaqua rock mouse (*Micaelamys namaquensis*), **Red veld rat** (*Aethomys chrysophilus*), **Highveld gerbil** (*Tatera brantsii*), **Spiny mouse** (*Acomys spinosissimus*), **Pygmy fieldmice** (*Apodemus microps*), **Yellow-necked wood mice** (*Apodemus flavicollis*) **House mice** (*Mus musculus domesticus*)	(Cavegn et al., 2013)	The numbers of Ki-67$^+$ and DCX$^+$ cells are similar for all the species with a habitat in southern Africa. Lower proliferation but higher neuronal differentiation in rodents from the southern African habitat compared to those from European environments.
		Long-tailed wood mice (*Apodemus sylvaticus*)	(Hauser et al., 2009)	No effect of voluntary running and environmental changes on the number of Ki-67$^+$ proliferative cells and DCX$^+$ immature neurons.
			(Cavegn et al., 2013)	The numbers of Ki-67$^+$ and DCX$^+$ cells are similar for all the species with a habitat in southern Africa. Lower proliferation but higher neuronal differentiation in rodents from the southern African habitat compared to those from European environments.
		Stella wood mouse (*Hylomyscus stella*), **Rwenzori striped mouse** (*Hybomys lunaris*), **Emin's pouched rat** (*Cricetomys emini*), **Beecroft's flying squirrel** (*Anomalurus beecrofti*), **Target rat** (*Stochomys longicaudatus*), **Yellow-spotted brush-furred rat** (*Lophuromys flavopunctatus*), **Natal mjultimammate rat** (*Mastomys natalesis*), **Lesser egyptian jerboa** (*Jaculus jaculus*), **Arabian spinny mouse** (*Acomys dimidiatus*), **Cairo spiny mouse** (*Acomys cahirinus*), **Wagner's gerbil** (*Gerbillys dasyurus*), **King jird** (*Meriones libycus*), **Libyan jird** (*Meriones libycus*), **Asian garden dormouse** (*Eliomys melanurus*). **Cape ground squirrel** (*Xerus inauris*)	(Patzke et al., 2015)	Presence of KI-67$^+$ proliferative cells and DCX$^+$ immature neurons in the SGZ and GCL.
	Carnivora	**Dog** (*Canis lupus familiaris*)	(Hwang et al., 2007)	Presence of DCX$^+$/NeuN$^-$ immature neurons with well-stained processes and located in the SGZ. Age-driven reduction in the number of DCX$^+$ cells.
			(Siwak-Tapp et al., 2007)	Reduction of BrdU$^+$ cells and DCX$^+$ immature neurons with age, which was not reversed by antioxidant-fortified food or behavioral enrichment in aged animals.
			(Pekcec et al., 2008)	Decrease of DCX$^+$ immature neurons and Ki-67$^+$ cells in the SGZ with age. No correlations between Aβ deposits and AHN.
			(De Nevi et al., 2013)	Presence of DCX$^+$ cells in the DG neurogenic region and reduction with age.

(Continues)

TABLE 1 (Continued)

Infraclass	Order	Species	Reference	Conclusions
			(Lowe et al., 2015)	Higher presence of DCX^+ and $DCX^+/NeuN^+$ neurons in the dorsal SGZ compared to the ventral DG.
			(Bekiari et al., 2020)	AHN was studied 14 and 30 days after BrdU administration, by using GFAP, DCX, CR, CB, NeuN and S100β markers. Higher numbers of resident DGCs, proliferating NSCs and $BrdU^+$ neurons in the dorsal DG. Newborn DGCs of the ventral DG showed prolonged differentiation, migration, and maturation.
		Red fox (*Vulpes vulpes*)	(Amrein et al., 2010)	Higher number of DCX^+ immature neurons in adult red foxes than in domesticated dogs but similar number to that in rodents. Extended maturation phase of immature neurons.
		American mink (*Neovison vison*)	(Malmkvist et al., 2012)	BrdU incorporation in the ventral DG. Increased number of $BrdU^+$ cells as stereotypic behavior increases.
		Ferret (*Mustela putorius furo*)	(Takamori et al., 2014)	Presence of $GFAP^+$ cells with long radial processes, $PCNA^+$ and $PH3^+$ proliferative cells, and DCX^+ immature neurons in the SGZ. DCX was co-expressed with PSA-NCAM, βIII-tubulin and B1 laminin.
			(Pillay et al., 2021)	DCX^+ neurons located at the inner border of the GCL and within the SGZ in both species. DCX^+ neurons exhibited apical dendrites that traversed the GCL to enter the ML.
		Feliform banded mongoose (*Mungos mungo*)	(Patzke et al., 2015)	Presence of DCX^+ cells with processes that extend into the ML and GCL.
			(Pillay et al., 2021)	DCX^+ neurons located at the inner border of the GCL and within the SGZ in both species. DCX^+ neurons exhibited apical dendrites that traversed the GCL to enter the ML.
		Asian small-clawded otter (*Aonyx cinerea*), **Harp seal** (*Pagophilus groenlandicus*), **Northern fur seal** (*Callorhinus ursinus*), **Siberian tiger** (*Panthera tigris altaica*) **African lion** (*Panthera leo*)	(Patzke et al., 2015)	Presence of DCX^+ cells with processes that extend into the ML and GCL.
		Silver fox (*Vulpes vulpes*)	(Huang et al., 2015)	Presence of $Ki67^+$ proliferative cells and DCX^+ immature neurons. Increased AHN in tameness-selected foxes in the middle and temporal hippocampal compartments. Similar proliferation but higher number of immature neurons in tameness-selected and unselected foxes as compared to rodents and primates.
	Chiroptera	**Pallas's long-tongued bat** (*Glossophaga soricina*), **Seba's short-tailed bat** (*Carollia perspicillata*), **Pale spear-nosed bat** (*Phyllostomus discolor*), **Egyptian slit-faced bat** (*Nycteris thebaica*), **Cyclops roundleaf bat** (*Hipposideros cyclops*), **Sundevall's roundleaf bat** (*Hipposideros caffer*), **Pseudoromicia rendalli** (*Neoromicia rendalli*), **Guinean pipistrelle bat** (*Pipistrellus guineensis*), **White-bellied house bat** (*Scotophilus leucogaster*), **Little free-tailed bat** (*Chaerephon pumila*), **Angolan free-tailed bat** (*Mops condylurus*)	(Amrein et al., 2007)	AHN was studied by means of the expresion of Ki-67, MCM2, DCX and NeuroD. AHN was present in *Chaerephon pumila*, *Mops condylurus* and *Hipposideros caffer*. In *Glossophaga soricina*, *Carollia perspicillata*, *Phyllostomus discolor*, *Nycteris macrotis*, *Nycteris thebaica*, *Hipposideros cyclops*, *Neoromicia rendalli*, *Pipistrellus guineensis*, and *Scotophilus leucogaster*, no positive cells were detected. Not all the antigens were recognized in all species.

TABLE 1 (Continued)

Infraclass	Order	Species	Reference	Conclusions
		Large-eared slit-faced bat (*Nycteris macrotis*)	(Amrein et al., 2007)	AHN was studied by means of the expresion of Ki-67, MCM2, DCX and NeuroD. No positive cells were detected. Not all the antigens were recognized in all species.
			(Chawana et al., 2014)	AHN was studied after euthanasia and perfusion following capture. Abundant number of DCX $^{+}$ cells in the DG in animals euthanized and perfused within 15 min of capture. Dramatic drop of AHN between 15 and 30 min post-capture, and absence of DCX^{+} immature neurons 30 min post-capture.
			(Patzke et al., 2015)	Presence of Ki-67^{+} proliferative cells and DCX^{+} immature neurons in the SGZ and GCL. The processes of the latter cells extended into the ML.
		Wahlberg's epauletted fruit bats (*Epomophorus wahlbergi*)	(Gatome et al., 2010)	Low, but persistent AHN in non-echolocating fruit bats. Incorporation of BrdU and expresion of PCNA, DCX and PSA-NCAM.
			(Chawana et al., 2013)	Ki-67^{+} and DCX^{+} cells in the SGZ and hilus.
			(Patzke et al., 2015)	Presence of Ki-67^{+} proliferative cells and DCX^{+} immature neurons in the SGZ and GCL. The processes of the latter cells extended into the ML.
		Franquet's epauletted fruit bat (*Epomops franqueti*) **Straw-colored fruit bat** (*Eidolon helvum*) **Hammer-headed fruit bat** (*Hypsignathus monstrosus*) **Short-palated fruit bat** (*Casinycteris argynnis*) **Woermann's fruit bat** (*Megaloglossus woermanni*) **Zenker's fruit bat** (*Scotonycteris zenkeri*)	(Chawana et al., 2013)	Ki-67^{+} and DCX^{+} cells in the SGZ and hilus.
			(Patzke et al., 2015)	Presence of Ki-67^{+} proliferative cells and DCX^{+} immature neurons in the SGZ and GCL. The processes of the latter cells extended into the ML.
		Egyptian fruit bat (*Rousettus aegyptiacus*)	(Chawana et al., 2013)	Presence of Ki-67^{+} and DCX^{+} cells in the SGZ and hilus.
			(Patzke et al., 2015)	Presence of Ki-67^{+} proliferative cells and DCX^{+} immature neurons in the SGZ and GCL. The processes of the latter cells extended into the ML.
			(Chawana et al., 2020)	Presence of Ki-67^{+} proliferative cells and DCX^{+} immature neurons in the DG of adult Egyptian fruit bats from three distinct environments: primary rainforest, subtropical woodland, and fifth-generation captive-bred. No differences in the numbers of proliferative cells, despite higher numbers of immature neurons in wild-caught bats.
		Trident leaf-nosed bat (*Asellia tridens*) **Kuhl's pipistrelle** (*Pipistrellus kuhlii*)	(Chawana et al., 2014)	AHN was studied after euthanasia and perfusion following capture. Abundant number of DCX $^{+}$ cells in the DG in animals euthanized and perfused within 15 min of capture. Dramatic drop of AHN between 15 and 30 min post-capture, and absence of DCX^{+} neurons 30 min post-capture.
		Sooty roundleaf bat (*Hipposideros fuliganosus*) **Persian trident bat** (*Triaenops persicus*) **Commerson's leaf-nosed bat** (*Hipposideros commersoni*) **Heart-nosed bat** (*Cardioderma cor*) **Little free-tailed bat** (*Chaerephon pumilus*) **African sheath-tailed bat** (*Coleura afra*) **Schreiber's long fingered bat** (*Miniopterus schreibersii*)	(Chawana et al., 2014)	AHN was studied after euthanasia and perfusion following capture. Abundant number of DCX $^{+}$ cells in the DG in animals euthanized and perfused within 15 min of capture. Dramatic drop of AHN between 15 and 30 min post-capture, and absence of DCX^{+} neurons 30 min post-capture.
			(Patzke et al., 2015)	Presence of Ki-67^{+} proliferative cells and DCX^{+} immature neurons in the SGZ. The processes of the latter cells extended into the ML and GCL.

(Continues)

TABLE 1 (Continued)

Infraclass	Order	Species	Reference	Conclusions
	Afrosoricida	**Hedgehog tenrec** (*Echinops telfairi*)	(Alpar et al., 2010)	Higher numbers of $BrdU^+$ and DCX^+ cells in the SGZ of younger than in aged animals. Gradual decrease of AHN with aging.
		Giant otter shrew (*Potamogale velox*)	(Patzke et al., 2013)	Presence of DCX^+ cells with strongly labeled proceses, presumably axons and dendrites, in the SGZ and GCL.
			(Patzke et al., 2015)	Presence of DCX^+ immature neurons in the SGZ and GCL. The processes of the latter cells extended into the ML.
		Hottentot golden mole (*Amblysomus hottentotus*)	(Patzke, LeRoy, et al., 2014)	Presence of DCX^+ immature neurons in the SGZ and GCL. The processes of the latter cells extended into the ML.
			(Patzke et al., 2015)	Presence of DCX^+ immature neurons in the SGZ and GCL. The processes of the latter cells extended into the ML.
	Primate (Prosimians)	**Demidoff's dwarf galago** (*Galagoides dmidoff*) **Bosman's potto** (*Perodicticus potto*) **Ring-tailed lemur** (*Lemur catta*)	(Patzke et al., 2015)	Presence of $Ki\text{-}67^+$ proliferative cells and DCX^+ immature neurons in the SGZ and GCL. The processes of the latter cells extended into the ML.
			(Fasemore et al., 2018)	Presence of $Ki\text{-}67^+$ proliferative cells and DCX^+ immature neurons in the SGZ.
		Gray mouse lemur (*Microcebus murinus*)	(Royo et al., 2018)	First evidence of the occurrence of AHN in prosimian primates. Increased number of newborn DGCs after n-3 PUFA supplementation for 21 months.
	Primate (Old World Primates)	**Vervet monkey** (*Chlorocebus pygerythrus*) **Olive baboon** (*Papio anubis*)	(Patzke et al., 2015)	Presence of DCX^+ immature neurons in the SGZ. The processes of the latter cells extended into the ML.
		Snow monkey (*Macaca fuscata*)	(Tonchev et al., 2003)	Incorporation of BrdU and DCX expression in control monkeys. Ischemic damage increased the number of BrdU-labeled cells. Newly generated cells expressed Musashi1, Nestin, βIII-tubulin, TUC-4, DCX, Hu, NeuN, S100β, or GFAP.
			(Tonchev et al., 2006)	BrdU incorporation in the adult DG. Ischemia increased the density of $BrdU^+$ cells. $BrdU^+$ newly generated cells showed neuronal features 79 days after the insult. Adult-born cells remained in the SGZ and showed immature progenitor phenotype.
		Long-tailed Macaque (*Macaca fascicularis*) **Rhesus monkey** (*Macaca mulatta*)	(Gould et al., 1999)	Incorporation of a substantial number of $BrdU^+$ cells in young adult and middle-aged monkeys. $BrdU^+$ cells showed morphological characteristic of immature and mature neurons and expressed TOAD, NSE, NeuN and CB. Few new cells expressed GFAP. Decrease in AHN in the oldest monkeys (23 years old) compared to younger animals.
			(Kornack et al., 1999)	Continuous generation of neurons, oligodendrocytes, and astrocytes. BrdU incorporation and expresion of TuJ1, NeuN, O4 and CNP. 10-fold decrease in AHN compared to the rates described in rodents.
			(Kohler et al., 2011)	Protracted DGC maturation in non-human primates over a minimum of 6 months. Expression βIII-tubulin, DCX, NeuN. Delayed dendritic arborization, and acquisition of mature cell body morphology.

TABLE 1 (Continued)

Infraclass	Order	Species	Reference	Conclusions
		Rhesus monkey (*Macaca mulatta*)	(Ngwenya et al., 2006)	Maturation sequence of adult primate DGCs is similar to that of adult rodents. $BrdU^+$ cells expressed TUC-4. Maturation lasts a minimum of 5 weeks.
			(Franjic et al., 2022)	Reconstruction of the entire AHN trajectory, from RGL cells to mature DGCs in the adult rhesus monkey. Profiling of 36,107 hippocampal nuclei using sn-RNA seq.
			(Wang et al., 2022)	Dissection of the whole AHN trajectory through the lifespan of the macaque, from NSC to mature DGCs. Profiling of 132,524 nuclei using sn-RNA seq. Macaque adult NSC features differed from those of rodents. Validation of ETNPPL as a NSC marker and that of STMN1 and STMN2 as immature neuron markers in primates.
		Long-tailed macaque (*Macaca fascicularis*)	(Hao et al., 2022)	Profiling of 207,785 cells from the adult macaque hippocampus using sc-RNA seq. Reconstruction of the whole AHN trajectory including a heterogeneous pool of RGLs, IPCs and neuroblasts. Identification of HMGB2 as a novel IPC marker. Differences with rodent AHN.
	Primate (New World Primates)	**Common marmoset** (*Callithrix jacchus*)	(Gould et al., 1998)	Production of new neurons in the DG of adult monkeys. Social stress-driven reduction in the number of proliferative cells.
			(Leuner et al., 2007)	BrdU incorporation and presence of DCX^+ and $PSA\text{-}NCAM^+$ immature neurons in the SGZ and GCL of young to middle-aged animals. Age-driven reduction in the number of $BrdU^+$ cells.
			(Bunk et al., 2011)	Presence of $Ki\text{-}67^+$ and DCX^+ cells. Age-dependent decline of AHN is associated with a decrease in the number of neuroblasts.
			(Marlatt et al., 2011)	BrdU incorporation and presence of DCX^+ immature neurons. Unchanged numbers of $BrdU^+$ or DCX^+ cells after 2 weeks of isolation and social defeat stress.
			(Amrein et al., 2015)	Presence of $Ki\text{-}67^+$ proliferative cells, $Tbr2^+$ intermediate precursor cells, $DCX^+/MCM2^+$ neuroblasts with proliferative potential, and DCX^+/CR^+ immature neurons. The limited co-expression of DCX and CR suggests an extended maturation phase. Age-related decrease in AHN.
		Squirrel monkey (*Saimiri sciureus*)	(Lyons et al., 2010)	BrdU incorporation in the DG. Increase in AHN after exposure to intermittent social separation and newpair formation. AHN positively correlated with the expression of genes involved in survival and integration of newly generated DGCs, as well as with enhanced spatial learning performance.
			(Patzke et al., 2015)	Presence of DCX^+ immature neurons in the SGZ. The processes of the latter cells extended into the ML.

(Continues)

TABLE 1 (Continued)

Infraclass	Order	Species	Reference	Conclusions
	Macroscelidea	**Eastern rock sengi** (*Elephantulus myurus*)	(Slomianka et al., 2013)	Captured sengis show fewer immature DCX$^+$ cells without changes in proliferative PCNA$^+$ cells than other murid species from the same habitat.
			(Patzke, LeRoy, et al., 2014)	Presence of DCX$^+$ immature neurons in the SGZ. The processes of the latter cells extended into the ML.
			(Patzke et al., 2015)	Presence of DCX$^+$ immature neurons in the SGZ. The processes of the latter cells extended into the ML.
		Four-Toed Sengi (*Petrodromus tetradactylus*)	(Patzke, LeRoy, et al., 2014)	Presence of DCX$^+$ immature neurons in the SGZ. The processes of the latter cells extended into the ML.
			(Patzke et al., 2015)	Presence of DCX$^+$ immature neurons in the SGZ. The processes of the latter cells extended into the ML.
	Hyracoidea	**Rock hyrax** (*Procavia capensis*)	(Patzke, LeRoy, et al., 2014)	Presence of DCX$^+$ immature neurons in the SGZ. The processes of the latter cells extended into the ML.
			(Patzke et al., 2015)	Presence of DCX$^+$ immature neurons in the SGZ. The processes of the latter cells extended into the ML.
	Proboscidea	**African elephant** (*Loxodonta africana*)	(Patzke, Olaleye, et al., 2014)	Presence of a moderate density of DCX$^+$ immature neurons in the SGZ and GCL. The processes of these cells extended into the ML.
			(Patzke et al., 2015)	Presence of DCX$^+$ immature neurons in the SGZ and GCL. The processes of these cells extended into the ML.
	Artiodactyla	**Pig** (*Sus scrofa*)	(Franjic et al., 2022)	Reconstruction of the whole AHN trajectory from RGL cells to mature DGCs in the young adult pig. Profiling of 36,851 hippocampal nuclei using sn-RNA seq.
		Swedish landrace pig (*Sus scrofa*), **Swedish farm sheep** (*Ovis aries*)	(Zhu et al., 2003)	Presence of RNR$^+$ proliferative cells in the SGZ. Morphological characterization of RNR$^+$ cells, which did not express markers of differentiated neurons or glial cells, except a fraction that co-expressed GFAP.
		Île-de-France sheep (*Ovis aries*)	(Brus et al., 2013)	BrdU incorporation and expression of DCX, NeuN, Sox2 and S100β. Longer maturation process than that in rodents and similar to that in non-human primates.
			(Levy et al., 2019)	Presence of Ki-67$^+$, Sox2$^+$, and DCX$^+$ cells. No effects of oxytocin on AHN.
		Sheep (*Ovis aries*)	(Piumatti et al.,2018)	BrdU incorporation and presence of Ki-67$^+$, DCX$^+$ and PSANCAM$^+$ cells in the adult sheep DG.
		Greater kudu (*Tragelaphus strepsiceros*) **Blue wildbeest** (*Connochaetes taurinus*) **Black wildbeest** (*Connochaetes gnou*) **Arabian camel** (*Camelus dromedarius*) **Affrican buffalo** (*Syncerus caffer*) **Nyala** (*Tragelaphus angasii*) **Common eland** (*Taurotragus oryx*) **Giraffe** (*Giraffa camelopardalis*) **Blesbok** (*Damaliscus pygargus*) **Springbok** (*Antidorcas marsupialis*) **Nubian ibex** (*Capra nubiana*)	(Patzke et al., 2015)	Presence of DCX$^+$ immature neurons in the SGZ and GCL. The processes of these cells extended into the ML.

TABLE 1 (Continued)

Infraclass	Order	Species	Reference	Conclusions
		Simitar-horned oryx (*Oryx dammah*) **Arabian oryx** (*Oryx leucoryx*) **Sand gazelle** (*Gazella marica*) **River hippopotamus** (*Hippopotamus amphibius*) **Domestic pig** (*Sus scrofa*)		
	Sirenia	**West Indian manatee** (*Trichechus manatus*)	(Patzke et al., 2015)	Presence of DCX^+ immature neurons in the SGZ and GCL. The processes of these cells extended into the ML.
	Cetacea	**Northern minke whale** (*Balaenoptera acutorostrata*), **Harbour porpoise** (*Phocoena phocoena*)	(Patzke et al., 2015)	Small hippocampus size of cetaceans compared to that of other mammals. Lack of DCX^+ cells in Northern minke whale and Harbour porpoise.
	Scandentia	**Tree shrews** (*Tupaia belangeri*)	(Gould et al., 1997)	Incorporation of BrdU in the SGZ. 3 weeks after injection, $BrdU^+$ NSE^+ cells with neuronal morphology were incorporated to the GCL. Presence of $Vimentin^+$ RGL cells with their processes extending into the GCL were observed in the SGZ. Negative and positive regulation of AHN by stress and NMDA receptor activation, respectively.

Note: This table was constructed after performing a manual search of studies that included the following terms (and their combination thereof) in the PubMed database: "Adult hippocampal neurogenesis", "mammal", "wild mammals", "cetacean", "non-human primate", "old world primate", "new-world primate", "non-placental mammal", "marsupialia", "carnivore", "herbivore", "primate", "chiroptera", "artiodactyla", "domestic animal", "eulipotyphla", "afrosoricida", "scandentia", "macroscelidae", "hyracoidea", "rodentia", "rodents", "didelmorphia", "pig", "sheep", "bat", "fox", "mole", "shrew", "rabbit", "wild rodent", "vole", "marine mammal", "prosimian", "sirenia", "elephant", "swine", "canis", "bovine", "ovine", "felis", "dolphin", "whale", and "seal." Studies not focused on the hippocampal region or that examined only human subjects were manually excluded.

Abbreviations: AHN, adult hippocampal neurogenesis; Aβ, amyloid-β; BrdU, 5-bromo-2′-deoxyuridine; CA3, cornu ammonis 3; CB, calbindin; CNP, 2′,3′-cyclic nucleotide phosphodiesterase; CR, calretinin; DCX, doublecortin; DG, dentate gyrus; DGC, dentate granule cell; ETNPPL, ethanolamine-phosphate phospho-lyase; GCL, granule cell layer; GFAP, glial fibrillary acidic protein; HMGB2, high-mobility group protein B2; IPC, intermediate progenitor cell; MCM2, minichromosome maintenance complex component 2; ML, molecular layer; n-3 PUFAS, n-3 polyunsaturated fatty acids; NeuN, neuronal nuclear antigen; NMDA, N-methyl-D-aspartate; NOS, nitric oxide synthase; NSC, neural stem cell; NSE, neuron-specific enolase; PCNA, proliferating cell nuclear antigen; PH3, phospho-histone H3; PSA-NCAM, polysialylated-neuronal cell adhesion molecule; RGL, radial glia-like; RNA, ribonucleic acid; RNR, ribonucleotide reductase; S100β, S100 calcium-binding protein β; Sc-RNA seq, single-cell RNA sequencing; SGZ, subgranular zone; Sn-RNA seq, single-nucleus RNA sequencing; Sox2, SRY-box transcription factor 2; Thymidine-H^3, tritiated thymidine; TOAD, turned on after division; TUC-4, turned on after division/ulip/CRMP-4; TuJ1, neuron-specific class III β-tubulin.

TABLE 2 List of studies addressing the occurrence of adult hippocampal neurogenesis (AHN) in humans

Study	Methods	Subject information	Tissue | PMD	Markers	Main results	Tissue processing	Quantification
(Eriksson et al., 1998)	IHC	Undisclosed sex (64.4 ± 2.9 years)	Postmortem | PMD not reported	BrdU, CB, NSE, GFAP, NeuN	Incorporation of BrdU into the adult human DG.	4% PFA for 24 h, sectioning on a sliding microtome.	Total number of $BrdU^+$ cells was determined in 5–7 sections from each subject. A semi-automatic image analysis system was used to estimate areas. Cell densities (cells/mm^3) were reported.
(Blümcke et al., 2001)	IHC	Controls (embryonic, postnatal and adult tissue), undisclosed age and sex. 11F/16M TLE (8 months–46 years)	Biopsy (TLE and Controls) and postmortem (Controls) | PMD controls (12 h– 3 d)	Nestin, Vimentin, Tuj1, Ki67, MAP1b/5, MAP2a-d, NF, NeuN, S100β, GFAP, Calbindin, CD68, CD45.	Increased neurogenesis in pediatric TLE patients. Delay in hippocampal maturation in a subgroup of TLE patients.	4% PFA for 24 h (biopsy) or formalin (undisclosed concentration) for ≥2 w (autopsies). Vibratome sectioning. Antigen retrieval for Ki67, MAP2a-d and Tuj1.	Positive cells were quantified in 5 regions of interest per DG using a semi-automated imaging analysis software. The same software was used to calculate the hippocampus area. Cell densities (cells/mm^2) were reported.
(Höglinger et al., 2004)	IHC	2F/1M Controls (87.7 ± 6.7 years), 2F/1M PD-NCI (71.3 ± 4.9 years), and 2F/3M PD-MCI (85.6 ± 5 years)	Postmortem | PMD controls (31.5 ± 7.2 h), PD-NCI (25.1 ± 8.2 h), and PD-MCI (19.4 ± 5.9 h)	Nestin, β-III Tubulin	The presence of $Nestin^+$ and β-III $Tubulin^+$ neural precursor cells is reduced in the SGZ of PD patients.	Tissue was dissected, fixed and frozen (undisclosed time and fixative). Sectioned in freezing microtome.	Cells were counted in the GCL and SGZ using a semi-automatic stereology system (ExploraNova Mercator) in regularly spaced sections. Cell densities (cells/mm^3) were reported.
(Jin et al., 2004)	IHC, WB	3F/8M Controls (46.09 ± 7.4 years), 1F/8M/4 undisclosed AD (76.22 ± 3.2 years)	Postmortem | PMD Controls (5–12 h) and AD (9–20 h)	DCX, PSA-NCAM, TUC4, NeuroD1	Increased expression of immature neuron markers in AD patients, measured by means of WB.	Frozen samples (WB), or 4% PFA (unknown fixation time) followed by paraffin embedding.	No quantifications are presented.
(Boekhoorn et al., 2006)	IHC	4F/6M Controls (67.1 ± 2.3 years) and 5F/4M AD (66.2 ± 2.0 years)	Postmortem | PMD Controls (9.7 h) and AD (5.1 h)	DCX, Ki67, GFAP	Comparison of optimal pH conditions during antigen retrieval for Ki67 detection. Unaltered number of $Ki67^+$ and DCX^+ cells in the DG of presenile AD cases.	10% formalin for 30–646 d. Paraffin-embedding and microtome sectioning. Antigen retrieval was performed for Ki67.	$Ki67^+$ cells were counted in 3–4 sections of each subject. Cell densities (cells/mm^2) were reported. For DCX and GFAP, a semi-quantitative approach was used.
(Reif et al., 2006)	IHC	15 Controls (48 ± 10 years), 15 SZ (44 ± 13 years), 15 BP (42 ± 12 years), and 15M DD (46 ± 9 years).	Postmortem | PMD Controls (23 ± 9 h), SZ (33 ± 14 h), BP (32 ± 16 h), and MDD (24 ± 11 h)	Ki67	Reduced number of $Ki67^+$ cells in SZ patients.	Frozen sections fixed in 4% PFA for 10 min.	$Ki67^+$ cells were counted in the GCL of 7 sections per patient. Cell densities (cells/mm) were reported.

TABLE 2 (Continued)

Study	Methods	Subject information	Tissue | PMD	Markers	Main results	Tissue processing	Quantification
		Sex of the subjects is not reported.					
(Manganas et al., 2007)	Magnetic resonance spectroscopy	5 healthy subjects (M, F). Three pre-adolescent (8–10 years) and 3 adolescent (14–16 years).	Living humans	Proton magnetic resonance spectroscopy (^{1}H-NMR)	Identification of NSCs in the adult human hippocampus. The presence of NSCs decreases with age.	-	Quantification of the signal amplitude (ppm).
(Monje et al., 2007)	IHC	Controls (10 months–63 years) and Cancer (10 months–61 years)	Postmortem | PMD controls and Cancer (<24 h)	DCX, Ki67, Olig2, CD68, CD20, CD3	AHN impairments and increased inflammation after cranial radiotherapy or systemic chemotherapy.	Undisclosed fixation protocol and duration. Embedding in paraffin.	The number of cells positive for each marker/total granule cell nuclei present in DG was reported.
(Verwer et al., 2007)	IHC, WB, RT-qPCR	5F/2M Controls (55–93 years), 15F/9M neurodegenerative diseases (AD, PiD, PSP, LBD, NAD, PD) (57–94 years), and 18F/11M Epilepsy (5–69 years)	Biopsy (Epilepsy) and postmortem (AD, PiD, PSP, LBD, NAD, PD and Controls) | PMD (9–48 h).	DCX, NeuN, GFAP	Presence of DCX$^+$ immature neurons in the hippocampus of AD patients.	Formalin-fixed tissue (undisclosed fixation time).	Semi-quantitative evaluation by means of a cellular profile scoring.
(Li et al., 2008)	IHC and ISH	9F/6M Controls (83.6 ± 7.4 years) and 7F/7M AD (79.4 ± 10.9 years)	Postmortem | PMD controls (2.6 ± 0.6 h) and AD (2.4 ± 0.6 h)	MAP2	Reduced expression of MAP2a,b (mature forms) in the DG of AD patients, which suggests impaired neuronal differentiation.	Fixation in 4% PFA for 24–48 h.	Optical density was measured.
(Liu et al., 2008)	IHC, WB, RT-PCR	5F/10M Controls (18–78 years) and 15F/9M TLE (13–57 years)	Biopsy (Blümcke et al.) and postmortem (Controls) | PMD controls (4.45–18.5 h)	DCX, PCNA, MCM2, PSA-NCAM, Tuj1, NeuN Reelin, CR, CB	The expression of DCX is increased in the hippocampus and temporal cortex of TLE patients. Co-expression of DCX and PCNA, Tuj1 and NeuN.	Perfusion/immersion in 15% formalin (undisclosed duration).	DCX$^+$ cells along the GCL were counted using the Stereoinvestigator software. Cell densities (cells/mm^3) were reported
(Boldrini et al., 2009)	IHC	3F/4M Controls (17–53 years), 1F/4M MDD (29–62 years), 1F/2M MDD/TCA (28–61 years), and 2F/2M MDD/SSRI (24–61 years)	Postmortem | PMD controls (9.5–22 h), MDD (4–22 h), MDD/TCA (9–19 h), MDD/SSRI (6–24 h)	Nestin, Ki67, NeuN, GFAP	Decreased number of NPCs with age. Increased number of NPCs in females. Antidepressant treatment increases the number of NPCs.	Frozen tissue, fixed in 4% PFA for 1w and sectioning in a freezing microtome.	Total number of cells positive for each marker was determined using the optical dissector and fractionator methods. The number of cells x 10^3 was shown.
(Mattiesen et al., 2009)	IHC	7F/12M Controls (35–81 years) and 9F/13M HIE (35–85 years)	Postmortem | PMD controls and HIE (0–5 d)	PCNA, TUC4, CR	Increased AHN and apoptosis after HIE. Aging did not impact on the number of proliferating or apoptotic cells in control subjects.	Formalin fixation (undisclosed time and concentration) and embedding in paraffin.	The number of cells positive for each marker was counted manually. Cell densities (cells/mm^2) were reported.
(Crews et al., 2010)	IHC, qRT-PCR, WB	3F/2M Controls (87 ± 4.6 years), 3F/4M Early AD (86.1 ± 1.7 years), and 4F/3M Severe AD (80 ± 1.9 years)	Postmortem | PMD controls (9.5 ± 3.5 h), early AD (11.8 ± 2.8 h), and severe AD (8.2 ± 0.8 h)	BMP6, DCX, Sox2	Increase in the expression of BMP6 and reduction in the number of DCX$^+$ and Sox2$^+$ cells in AD patients.	Formalin (undisclosed concentration) or 4% PFA (undisclosed duration). Vibratome sectioning.	The number of cells positive for each marker was counted in every sixth section and were multiplied by the

(Continues)

TABLE 2 (Continued)

Study	Methods	Subject information	Tissue | PMD	Markers	Main results	Tissue processing	Quantification
							reference volume. Total number of cells was reported.
(D'Alessio et al., 2010)	IHC	3F/2M Controls (45.8 ± 14 years) and 6F/3M TLE (40.1 ± 6 years)	Biopsy (Blümcke et al.) and postmortem (Controls) | PMD not reported.	DCX	Reduced number of DCX^+ cells in patients with TLE.	Formalin for 5 d (undisclosed concentration) and embedding in paraffin. Microtome sectioning.	The number of cells positive for each marker was determined by computerized image analysis. Ten fields per section were evaluated. Cell densities (cells/field) were reported.
(Geha et al., 2010)	IHC	3F/2M Surgical Controls (25–66 years), 2F/3M Autopsy Controls (31–64 years), and 6F/4M TLE (22–35 years)	Biopsy (epilepsy and surgical controls) and postmortem (controls) | PMD not reported	Ki67, MCM2, Mib-1, Tuj1, MAP2, NeuN, Calretinin, GFAP, Nestin, Olig2, NG2.	Fixation time affects the detection of cell cycle-related proteins. Patients with TLE show increased numbers of $Ki67^+$ cells in the SGZ, which acquire glial phenotypes.	Formalin-zinc (formalin 5%; zinc 3 g/L; sodium chloride 8 g/L) for 3 months (postmortem) or 16 h (surgical), and embedding in paraffin.	Cells were counted manually for each of the 10 tissue blocks that made up each hippocampal resection. Cell densities (cells/mm^2 or cells/cm^2) were reported.
(Hong et al., 2010)	IHC	Undisclosed	Undisclosed	DCX, p-TAU (PS396, PT231, PT205).	Colocalization between DCX and p-Tau in patients with AD.	Undisclosed fixation procedure. Freezing microtome sectioning.	-
(Knoth et al., 2010)	IHC, ISH, WB	28F/22M adult (1 d–100 years) and fetal (11, 20, and 40 gw) Controls	Postmortem | PMD: 1–60 h	DCX, PCNA, Ki67, MCM2, Sox2, Nestin, TUC4, Tuj1 Prox1, PSA-NCAM, GFAP, Calretinin, NeuN.	Human AHN shares features identified in rodents. Mild decrease of AHN with age.	Formalin fixation (undisclosed duration and concentration). Paraffin embedding.	DCX^+ cells were counted manually in 3 sections of the anterior hippocampus of each patient. The average number of positive cells/mm^2 per 3 sections was given.
(Lucassen et al., 2010)	IHC	3F/7M Controls (48–85 years) and 3F/7M MD (45–84 years)	Postmortem | PMD controls (4–19.15 h) and MD (4–28 h)	MCM2, PH3	Reduction in the number of $MCM2^+$ cells in MD patients.	4% Formaldehyde for 4–5 w and embedding in paraffin.	The number of cells positive for each marker was quantified in 5–6 sections. Cell densities (cells/μm^2) were reported.
(M. Johnson et al., 2011)	IHC	5F/3M Controls (71–101 years) and 3F/5M LBD (75–84 years)	Postmortem | PMD controls (12–84 h) and LBD (51–96 h)	PCNA, GFAP, Musashi, DCX, Nestin, α-synuclein, Aβ	Loss of Musashi and GFAP. Increase in PCNA in the SGZ and GCL, and in the number of DCX^+ cells in the GCL of patients with LBD.	Undisclosed fixation protocol. Embedding in paraffin. Microtome sectioning. Antigen retrieval.	The percentage of stained area was analyzed in 5 random images of each region. In addition, DCX^+ cells were counted in the whole DG. Data were represented as the percentage of stained area per total area measured.

TABLE 2 (Continued)

Study	Methods	Subject information	Tissue | PMD	Markers	Main results	Tissue processing	Quantification
(Low et al., 2011)	IHC	1F/7M Controls (32–81 years) and 5F/9M HD (35–75 years)	Postmortem | PMD controls (9–24 h) and HD (3–24 h)	PCNA, Bcl-2, MCM2, Musashi	No differences in SGZ proliferation between control subjects and HD patients.	Perfusion and 24 h fixation with 15% formalin. Microtome sectioning. Antigen retrieval.	Cells were counted manually. Cell density was reported as average number of positive cells per 50 μm, per μm^2, and per mm of hippocampal section.
(Winner et al., 2012)	IHC	3F/3M Controls (86.00 ± 10 years) and 1F/5M LBD (81.0 ± 9.1 years).	Postmortem | PMD controls (12.8 ± 7.2 h) and LBD (9.5 ± 3.1 h)	Sox2, α-synuclein, DCX	Increased α-synuclein and decreased numbers of $Sox2^+$ cells in patients with LBD.	Fixation in 4% PFA (undisclosed duration).	The optical dissector method was used to count positive cells. The reference volume was determined using Stereoinvestigator MicroBrightField software. 3 systematically sampled sections (10 images per section) were analyzed to estimate the average number of immunolabeled cells/mm^2.
(Boldrini et al., 2012)	IHC	7F/5M Controls (41.8 ± 14.6 years), 6F/6M MDD (43.6 ± 13.3 years), 4F/2M MDD/TCA (46.2 ± 17.1 years), and 2F/2M MDD/SSRI (38.8 ± 13.8 years)	Postmortem | PMD controls (15.3 ± 4.8 h), MD (16.0 ± 5.9 h), MD/TCA (12.1 ± 5.2 h), and MD/SSRI (15.8 ± 7.5 h)	Ki67, Nestin, PECAM, Collagen IV	Decreased number of $Nestin^+$ cells with age. SSRI treatment increases the number of $Nestin^+$ cells in the DG of MD patients.	4% PFA (undisclosed duration) and freezing. Freezing microtome sectioning.	The number of positive cells, area occupied by capillaries, and the volume and length of the DG, CA1 and parahippocampal gyrus were calculated using the optical dissector and fractionator methods. Total number of cells was reported.
(Perry et al., 2012)	IHC	13F/8M Controls (80.9 ± 8.5 years) and 13F/7M AD (81.2 ± 7 years)	Postmortem | PMD not reported	Musashi, Nestin, PSA-NCAM, DCX, Tuj1, ChAT	Reduced immunoreactivity of Musashi and ChAT, and increased immunoreactivity of $Nestin^+$ and $PSA\text{-}NCAM^+$ in AD. Higher levels of DCX in the GCL of AD patients. No changes in Tuj1.	4% Formaldehyde for 4 w and embedding in paraffin. Microtome sectioning. Antigen retrieval	A threshold was established to detect immunopositive signal. The integrated optical density was reported.
(Epp et al., 2013)	IHC	4F/8M Controls (46.8 ± 3.49 years), 5F/7M MDD (42.83 ± 2.92 years), and 6F/6M MDD-psychosis (41.5 ± 3.47 years)	Postmortem | PMD not reported	DCX, p21, NeuN	Increased number of DCX^+/NeuN cells in patients with depression.	Frozen tissue, cryosectioned and fixed in 4% formaldehyde for 15 or 45 min.	The number of cells was counted in the GCL and SGZ of each section. Cell densities (cells/mm^2) or the total number of NeuN cells

(Continues)

TABLE 2 (Continued)

Study	Methods	Subject information	Tissue | PMD	Markers	Main results	Tissue processing	Quantification
							per subject within the region of interest were reported.
(Spalding et al., 2013)	C^{14} dating	32F/88M Controls (16–92 years)	Postmortem | PMD not reported	C^{14} incorporation	Mild decrease in AHN with aging. 700 new neurons are added daily to the human DG.	Frozen tissue. Homogenized for nuclei isolation.	The rate of new neurons added into the human DG was calculated by retrospectively birth dating cells (ΔC^{14}) and a mathematical model based on cell death rate, and the fractions of renewing and non-renewing cells.
(Ernst et al., 2014)	IHC, WB	4 (undisclosed sex) Controls (20–71 years)	Postmortem | PMD not reported	DCX, PSA-NCAM, MAP2, IdU, caspase-3	Expression of immature neuron markers, as well as IdU incorporation in the SGZ.	Frozen tissue, sectioned by cryostat and fixed in 2% formaldehyde for 10 min. For IdU, formalin-fixed (undisclosed protocol) and embedding in paraffin sections were used. Antigen retrieval.	Undisclosed.
(Gomez-Nicola et al., 2014)	IHC	5F/5M Controls for CJD variant (20–35 years), 4F/5M Controls for AD (58–79 years), 5F/5M CJD variant(20–34 years), and 5F/5M AD (58–76 years)	Postmortem | PMD not reported	Ki67, Sox2, CR	Increased number of $Ki67^+$ and CR^+, but no changes in that of $Sox2^+$ cells in patients with AD and CJD variant. Decreased numbers of these cell populations in aged controls.	Formalin-fixation (undisclosed protocol) and embedding in paraffin. Antigen retrieval.	The number of positive cells was counted in 4–5 fields per DG sample using ImageJ. Cell densities (cells/mm^2) were reported.
(Bayer et al., 2015)	IHC	6F/22M Controls (17–41 years) and 8F/12M heroin users (17–45 years)	Postmortem | PMD controls (2.4 d) and heroin users (2.6 d)	Musashi, Nestin, Ki67, CR, GFAP, NeuN, Tuj1, DCX	Reduced number of $Musashi^+$ and $Nestin^+$ progenitor and proliferating cells in heroin users.	Fixation in 4% formaldehyde for 48 h-5 years, embedding in paraffin and microtome sectioning. Antigen retrieval.	The number of positive cells was counted manually in at least 3 fields of the GCL, SGZ and CA4. Total cell numbers, percentage of positive cells/total cell numbers, and cell densities (cells/mm^2) were reported.
(D'Alessio et al., 2015)	IHC	4F/4M Controls (23–60 years) and 7F/9M TLE (22–51 years)	Biopsy (Blümcke et al.) and postmortem (Controls) | PMD not reported	Nestin	Reduced number of $Nestin^+$ cells in patients with epilepsy.	Formalin-fixation (undisclosed concentration) for 5 d, embedding in paraffin and microtome sectioning.	The number of $Nestin^+$ cells, mean gray value and reactive area (px^2) were determined along the GCL in 10 fields per section.

TABLE 2 (Continued)

Study	Methods	Subject information	Tissue | PMD	Markers	Main results	Tissue processing	Quantification
(Ekonomou et al., 2015)	IHC	5F/7M Braak-Tau stages 0-II (80.3 ± 8.4 years), 8F/3M Braak-Tau stages III-IV (88.9 ± 8.2 years), and 1F/4M Braak-Tau stages V-VI (86.8 ± 5.3 years)	Postmortem | PMD Braak-Tau stages 0–II (12–28 h), Braak-Tau stages III-IV (7–27 h), and Braak-Tau stages V-VI (9.5–33 h)	HuC/HuD, Nestin, PCNA, GFAP, Iba1	Reduced number of HuC/HuD$^+$ cells in patients at Braak-Tau V-VI stages. Increased presence of DCX$^+$ cells in patients with dementia at advanced Braak-Tau stages.	Undisclosed fixation protocol. Paraffin embedding. Antigen retrieval.	The hippocampus area was measured on each section. Cell densities (cells/mm) were reported.
(Allen et al., 2016)	IHC	3F/13M Controls (21–81 years) and 5F/5M SZ (55–75 years)	Postmortem | PMD controls (10–50 h) and SZ (12.5–72 h)	Ki67, NeuN	Reduced number of Ki67$^+$ cells in patients with SZ.	Frozen tissue, fixed in 4% PFA for 10 min at 4°C.	The density of Ki67$^+$ (number of cells/mm^2) within the SGZ, GCL and hilus was calculated in 3 slides per case. Stereoinvestigator was used to measure the area on each section.
(Dennis et al., 2016)	IHC	9F/14M Controls (0.2–59 years)	Postmortem | PMD controls (15–90 h)	Ki67, DCX, Tuj1, Olig2, EGFR, GFAP, PCNA	Marked decrease in proliferation and neuroblasts with age. Among the proliferating cell population, only microglial cells were identified	15–20% formalin-fixation for 2–3 w. Paraffin embedding. Antigen retrieval.	Ki67$^+$, DCX$^+$ and PCNA$^+$ cells were counted within the entire SVZ and SGZ of each section. Cell densities (cells/mm^2) were reported.
(Galan et al., 2017)	IHC	1F/3M Controls (69.50 ± 11.38 years) and 4F/5M ALS (65.60 ± 15.94 years)	Postmortem | PMD controls and ALS (5 ± 2 h)	Ki67, PCNA, GFAPδ, PSA-NCAM, DCX, Tuj1, GFAP, TDP43	Proliferation and PSA-NCAM$^+$ markers in the SGZ were decreased in patients with ALS.	Undisclosed fixation protocol. Paraffin embedding and vibratome sectioning. Antigen retrieval.	Cells were counted in ~10 fields for each marker. Cell densities (cells/500 μm^2) were reported.
(Mathews et al., 2017)	qPCR, IHC	4F/22M Controls for qPCR and 1F/4M Controls for IHC (18–88 years)	Postmortem | PMD controls (9–51 h)	Ki67, DCX, GFAPδ, GFAP, Tbr2	Reduced DCX and Ki67 mRNA expression with aging.	Dissected and fresh frozen tissue (qPCR). Formalin-fixed (undisclosed fixation protocol) and embedded in paraffin (IHC).	3 randomly selected areas of the hilus were photographed for visual analysis. No cell density values were reported.
(Oreja-Guevara et al., 2017)	IHC	1M Control (undisclosed age) and 1M MS (27 years)	Postmortem | PMD not reported	GFAPδ, Musashi, Sox2, Pax6, NG2, Ki67, PCNA, Iba1, CD68, MHCII, Tuj1, DCX, PSA-NCAM, MBP, AQ4, Nestin, Olig	Low numbers of NSCs, intermediate progenitors and proliferation. Early AHN impairments in MS.	Fixation in 4% PFA (undisclosed time), paraffin embedding, and microtome sectioning. Antigen retrieval.	8 random images from each section were analyzed. Cell densities (cells/mm^2 or cells/mm) were reported.
(Liu et al., 2018)	IHC	5 Developmental Controls (12–13 gw), 6F/9M Adult Controls (28–75 years), and 20F/22M Epilepsy (8–76 years)	Biopsy (epilepsy) and postmortem (Controls and epilepsy) | PMD not reported	Nestin, DCX, Musashi, Tuj1, NeuN, GFAPδ, MAP2, Olig2, MCM2, AQ4, GS, ZnT3, CD34	Increased densities of Nestin$^+$ cells in patients with epilepsy.	Formalin-fixed (undisclosed protocol) and embedding in paraffin.	Semi-quantitative evaluation of the number of Nestin$^+$ cells. No cell density values were reported.

(Continues)

TABLE 2 (Continued)

Study	Methods	Subject information	Tissue | PMD	Markers	Main results	Tissue processing	Quantification
(Le Maitre et al., 2018)	IHC	6F/11M Controls (24–78 years) and 1F/17M Alcohol consumers (30–67 years)	Postmortem | PMD controls (11.25–84.5 h) and Alcohol consumers (5.25–64 h)	NeuN, DCX, Sox2, Ki67	Reduction of AHN markers in alcohol consumers.	Flash-frozen tissue, fixed in 4% formaldehyde for 15–30 min and cryosectioned.	Positive cells for each marker were counted along the entire length of the GCL in the DG, in 5 sections/case. Cell densities (cells/mm^2) were reported.
(Boldrini et al., 2018)	IHC	11F/17M Controls (14–79 years)	Postmortem | PMD controls (4–26 h)	PSA-NCAM, Sox2, Nestin, Ki67, DCX, NeuN, GFAP	Preserved numbers of intermediate progenitors and immature neurons, and decrease in quiescent progenitors throughout aging.	Flash-frozen tissue, fixed in 4% PFA (undisclosed duration) and microtome sectioning.	10–12 sections per subject were analyzed along the rostro-caudal axis of the hippocampus. The optical dissector with fractionator approach was used with Stereoinvestigator software to estimate total cell numbers in the selected region
(Cipriani et al., 2018)	IHC	39 Controls (13 gw–72 years) and 5 AD (74–89 years). Undisclosed sex.	Postmortem | PMD controls (4–72 h, 27 subjects undisclosed) and AD (3–23 h)	Nestin, GFAP, DCX, Ki67, MCM2, Sox2, Pax6, Tbr2, Vimentin, Tuj1.	Reduction of RGL, proliferative, and DCX$^+$ cells in the adult human DG.	Frozen tissue was fixed in 4% PFA (undisclosed duration), embedded in paraffin and cryosectioned.	Semi-quantitative analysis. No cell densities or numbers were reported.
(Sorrells et al., 2018)	IHC, EM	13F/24M Controls (14 gw–77 years) and 11F/11M Epilepsy (3 m–64 years)	Biopsy (epilepsy) and postmortem (controls) | PMD controls (<48 h)	Ascl1, BLBP, DCX, BrdU, GFAP, Hopx, Ki67, MCM2, Nestin, NeuN, NeuroD, Olig2, Pax6, Prox1, PSA-NCAM, Sox1, Sox2, Tbr2, Tuj1, Vimentin, Iba1	Absence of AHN markers in the adult human DG.	Perfusion with 4% PFA, fixation in either 4% PFA or 10% formalin (undisclosed duration). Additional fixation in 4% PFA for 2 days.	Quantification of 3–5 images across a minimum of 3 randomly selected sampled sections for each age. The DG was subdivided into subregions of interest (GCL, hilus and ML). Cell densities (cells/mm^2) and total cells/section were reported.
(Stepien et al., 2018)	IHC	2F/6M Controls (64 ± 10.95 years), 7F/7M Non-hemorrhagic stroke (70 ± 6.03 years), and 2F/6M Hemorrhagic stroke (64.75 ± 12.23 years)	Postmortem | PMD not reported	GFAP, PH3	Presence of neural stem cells and NPCs observed in the DG and SVZ. Increased number of PH3$^+$ cells in patients with hemorrhagic stroke.	Undisclosed fixation protocol and embedding in paraffin. Rotary microtome sectioning. Antigen retrieval.	Quantitative analysis was performed using the CellSens software. Cells were counted in the DG and SVZ. Cell densities (cells/mm^2) were reported.
(Tartt et al., 2018)	IHC, ISH, RNAscope	5 Controls, 5 antidepressant-treated, and 5 untreated subjects with MDD (19–67 years). Undisclosed sex.	Postmortem | PMD control, antidepressant-treated, and untreated MDD patients (6–27 h)	DCX, NF, Sox2, PSA-NCAM, NeuN	Detection of AHN markers by means of RNAscope.	Flash-frozen tissue. Undisclosed fixation protocol.	Cells expressing DCX mRNA were quantified in 3 sections of the anterior-mid DG. Cell densities (cells/mm^3) were reported.

TABLE 2 (Continued)

Study	Methods	Subject information	Tissue | PMD	Markers	Main results	Tissue processing	Quantification
(Gatt et al., 2017)	IHC	15 Controls (80.47 ± 8.48 years) and 41 LBD/PDD (79.98 ± 5.32 years). Sexes were equally represented (52% F 48% M).	Postmortem | PMD controls (34.26 ± 17.32 h) and LBD/PDD (36.30 ± 25.51–49.95 ± 21.57 h)	DCX	Increased presence of DCX^+ immature neurons in the SGZ of patients with LBD/PDD. Higher expression of DCX in patients treated with SSRI. Higher DCX expression corelated with higher cognitive scores.	Undisclosed fixation protocol. Paraffin-embedded tissue. Antigen retrieval.	DCX^+ cells were counted throughout the entire DG. Cell densities (cells/mm) were reported.
(Gomez-Pinedo et al., 2019)	IHC	4 (undisclosed sex) Controls and 5F/7M MND (ALS or ALS-FTD) (37–87 years).	Postmortem | PMD controls and ALS (2–6 h)	PCNA, Ki67, GFAPδ, PSA-NCAM, DCX, Tuj1, Iba1, Nestin	Decrease in the proliferative and neurogenic activity, and number of $GFAP\delta^+$ cells and neuroblasts in patients with ALS.	Samples were fixed with 10% formalin-(undisclosed time), embedded in paraffin, and microtome sectioned. Antigen retrieval.	The number of cells was determined in 5 slides per patient with 32 fields/slide (CA1, CA2, CA3 and DG). ImageJ was used to measure optical density. The relative number of inclusions was divided by the mean number of neurons per field (cells/mm^2).
(Moreno-Jimenez et al., 2019)	IHC	4F/9M Controls (43–87 years) and 19F/26M AD (52–97 years)	Postmortem | PMD controls (3–38 h) and AD (2.5–10 h)	DCX, PH3, GFAP, Prox1, Tau, NeuN, CR, CB, Tuj1, PSA-NCAM, Aβ	Persistence of AHN markers in neurologically healthy control subjects, mild decrease in AHN with aging, and sharp decrease in AD patients.	Fixed in 4% PFA for 24 h. Vibratome sectioning. Mild and optimized antigen retrieval (limited number of microwave cycles avoiding boiling, 20 min in a commercial citrate buffer at 80°C).	The number of cells was estimated using the physical dissector method adapted to confocal microscopy. Cells were counted on 5–20 stacks of images obtained from 10 sections/subject. The number of cells was divided by the reference volume of the GCL in each image. Cell densities (cells/mm^3) were reported.
(Seki et al., 2019)	IHC	6M Controls (16–49 years) and 4F/8M Epilepsy (9–43 years)	Biopsy	PSA-NCAM, Ki67, HuB, DCX, GFAP	Reduced numbers of $Ki67^+$/HuB^+/DCX^+ cells in the adult DG.	Fixed in 4% PFA for 3 d and frozen; cryostat sectioning. Antigen retrieval.	The number of cells positive for each marker in the GCL was counted in 2–5 sections/subject. Cell densities (cells/mm^2) were reported.
(Tobin et al., 2019)	IHC	3F/3M Controls (79–93 years) and 11F/1M AD (85–99 years)	Postmortem | PMD controls (4.92–20.17 h) and AD (4.42–43.55 h)	DCX, PCNA, Nestin, Sox2, Ki67	Persistence of AHN markers during aging and AD patients. AHN correlated with cognitive scores.	Undisclosed fixation method. Paraffin embedding. Antigen retrieval.	Cell counts were calculated in 2–4 sections/subject using the optical fractionator workflow of StereoInvestigator. Cell

(Continues)

TABLE 2 (Continued)

Study	Methods	Subject information	Tissue | PMD	Markers	Main results	Tissue processing	Quantification
							densities (cells/mm^3) or total cell numbers were reported.
(Flor-Garcia et al., 2020)	IHC	4F/9M Controls (43–87 years)	Postmortem | PMD controls (3–38 h)	DCX, NeuN, PSA-NCAM, MAP2, CB, Prox1, CR, PH3, GFAP, Tuj1, Tau, S100β	Reduced expression of NeuN in DCX$^+$ cells as compared to fully mature DGCs.	4% PFA for 24 h and vibratome sectioning. Mild and optimized antigen retrieval (limited number of microwave cycles avoiding boiling, 20 min in a commercial citrate buffer at 80°C).	A modified physical dissector method coupled to confocal microscopy was used to quantify cell densities inside a reference volume. The number of cells was divided by the reference volume of the GCL in each image. Cell densities (cells/mm^3) were reported.
(Terreros-Roncal et al., 2021)	IHC	5F/10M Controls (43–87 years), 6F/6M ALS (48–80 years), 2F/4M HD (47–72 years), 6M DLB (62–89 years), 1F/2M PD (73–82 years), and 2F/4M FTD (56–87 years)	Postmortem | PMD controls (3–38 h), ALS (5–12 h), HD (6–17 h), DLB (3–10 h), PD (5–10 h), and FTD (3.5–12 h)	S100β, DCX, Nestin, Sox2, PH3, HuC/HuD, PSA-NCAM, CR, NeuN, CB, Iba1, pTau, Tau3R, UEA1, htt, pTDP43, α-synuclein	In patients with neurodegenerative diseases, adult-born DGCs show abnormal morphological development and changes in the expression of differentiation markers. Ratio of quiescent to proliferating hippocampal neural stem cells shifts, and homeostasis of the neurogenic niche is altered.	Samples were fixed in 4% PFA for 24 h, included in 10% sucrose-4% agarose and vibratome-sectioned. Mild and optimized antigen retrieval (limited number of microwave cycles avoiding boiling, 20 min in a commercial citrate buffer at 80°C).	The number of cells was estimated by using the physical dissector method adapted to confocal microscopy. Cells were counted on 5–20 stacks of images obtained from 5–10 sections/subject. The number of cells was divided by the reference volume of the GCL in each image. Cell densities (cells/mm^3) were reported.).
(Franjic et al., 2022)	IHC; snRNA-seq	2F/4M Controls for snRNA-seq (44–79 years), 3F/3M Controls for IHC (38–76 years), and 3F/11M AD for IHC (61–89 years)	Postmortem | PMD controls (2–26.1 h) and AD (8–28 h)	DCX, GAD1, METL7B	Absence of AHN transcriptomic and histological signatures.	Frozen tissue for snRNA-seq. Fresh tissue for IHC, fixed with 4% PFA/PBS (undisclosed duration) followed by 30% sucrose/PBS. High intensity antigen retrieval (20 min in citrate buffer pH 6 at 95°C) for DCX. No antigen retrieval for PSA-NCAM detection.	Undisclosed quantification protocol.
(Ammothumkandy et al., 2022)	IHC	3F/6M Controls (21–56 years) and 12F/6M TLE (20–56 years)	Postmortem | PMD controls and TLE (6–23 h)	Arc, DCX, c-fos, Ki67, GAD65/67 GFAP, Iba1, Prox1, PSA-NCAM, S100ß, Tuj1, GluR2/3	Longer duration of epilepsy is associated with a sharp decline in neuronal production.	Fixation in 4% PFA (12 h per mm of tissue thickness) and microtome sectioning.	Quantifications were performed manually on Zeiss blue software. The GCL boundaries were determined using the DAPI channel. Cells

TABLE 2 (Continued)

Study	Methods	Subject information	Tissue | PMD	Markers	Main results	Tissue processing	Quantification
							were counted in the whole section. Cell densities (cells/mm^3) were reported.
(Wang et al., 2022)	snRNA-seq, IHC	2F/4M Controls (52–92 years)	Postmortem | PMD controls (5–22.7 h)	PCNA, PAX6, Sox2, ETNPPL, NEUROD1, STMN1, STMN2, CB, Ki67, DCX, NeuN, Ascl1, HES6, Prox1, NNAT.	Presence of AHN transcriptomic and histological signatures such as proliferative NSCs, and immature neuron markers.	Blocks were either frozen in liquid nitrogen (snRNA-seq) or fixed overnight in 4% PFA at 4°C (IHC). Sectioned by cryostat. Antigen retrieval.	No quantification protocol reported. Images obtained by confocal microscopy and analyzed with ImageJ software. Cell densities (cells/mm^2) were reported.
(Zhou et al., 2022)	snRNA-seq, IHC, in vitro slice culture	Sn-RNAseq: 0–2 years, 3M/1F; 3–6 years, 2M/2F; 13–18 years, 2M/2F; 40–60 years, 4M/1F; 86–92 years, 2M/3F; AD, 73–88 years, 4M/4F; and matched controls, 73–88 years, 6M/2F. IHC: 16M/8F (20 gw– 64 years) Slice culture: 5M/5F (2–61 years)	Biopsy (slice culture) and Postmortem | PMD sn-RNAseq: 2.3–44 h. IHC: 5.9–43 h.	ATF4, CB, Caspase 3, DCX,Iba1, Math3, Ki67, NeuN, NEUROD1, NFIA, OLIG2, OP18, Prox1, S100β, STMN1, Tbr2.	Presence of immature neurons and proliferative progenitors in the human DG. In vitro EdU incorporation. Low-frequency proliferation and extended maturation. Decreased number of immature DGCs in patients with AD.	Blocks were fixed in 4% PFA at 4°C for 24–48 h and cryoprotected. Forty-μm sections obtained in a frozen sliding microtome. A small proportion of the blocks was formalin-fixed and paraffin-embedded. Incubation with 0.5% NaBH4 for 30 min. Antigen retrieval with target-retrieval solution (DAKO).	PROX1$^+$ DGCs or DAPI$^+$ cells were counted by semi-automated nuclear staining quantification using Fiji. SGZ and GCL were delineated using Prox1 staining. No quantification protocol reported for other cell counts.

Note: This table was constructed after performing a manual search of studies that included the following terms (and their combination thereof) in the PubMed database: "Adult hippocampal neurogenesis," "human," and "new neurons." Studies not focused on the human hippocampal region or that examined only other species were manually excluded.

Abbreviations: AD, Alzheimer's disease; AHN, adult hippocampal neurogenesis; ALS, amyotrophic lateral sclerosis; AQ4, aquaporin-4; Ascl1, Achaete-Scute family BHLH transcription factor 1; ATF4, activating transcription factor 4; BLBP, brain lipid-binding protein; BP, bipolar disorder; BrdU, bromodeoxyuridine; CB, calbindin; CJD, Creutzfeldt-Jakob disease; CR, calretinin; DCX, doublecortin; DG, dentate gyrus; DGCs, dentate granule cells; DLB, dementia with Lewy bodies; DMSO, dimethyl sulfoxide; EGFR, epidermal growth factor receptor; EM, electron microscopy; F, female; FTD, frontotemporal dementia; GAD1, glutamate decarboxylase 1; GCL, granule cell layer; GFAP, glial fibrillary acidic protein; Gw, gestational weeks; HD, Huntington's disease; HIE, hypoxic–ischemic encephalopathy; Hopx, homeodomain-only protein homeobox; HSV, hue, saturation and value; Iba1, ionized calcium-binding adaptor molecule 1; ICH, immunohistochemistry; ISH, in situ hybridization; LWB, Lewy body dementia; M, male; MAP2, microtubule-associated protein 2; MBP, myelin basic protein; MCM2, minichromosome maintenance complex component 2; MD, major depression; MDD, major depressive disorder; MDD/SSRI, MDD with selective serotonin reuptake inhibitor; MDD/TCA, MDD with tricyclic antidepressant; METTL7B, methyltransferase-like protein 7B; MHCII, major histocompatibility complex II; MND, motor neuron disease; MRI, magnetic resonance imaging; MS, multiple sclerosis; MTLE, mesial temporal lobe epilepsy; NeuN, neuronal nuclear antigen; NeuroD1, neuronal differentiation 1; NF1A, nuclear factor I a; NG2, neural-glial antigen 2; NPCs, neural progenitor cells; NSCs, neural stem cells; Olig2, oligodendrocyte transcription factor 2; OP18, stathmin; PAX6, paired box 6; PBS, phosphate saline buffer; PCNA, proliferating cell nuclear antigen; PD, Parkinson's disease; PDD, Parkinson's disease with dementia; PD-MCI, Parkinson's disease mild cognitive impairment; PD-NCI, Parkinson's disease non-cognitive impairment; PFA, paraformaldehyde; PH3, phospho-histone 3; PLI, polarized light imaging; PLP, proteolipid protein; PMD, postmortem delay; Prox1, prospero homeobox 1; PSA-NCAM, polysialylated-neural cell adhesion molecule; pTau, phospho-tau; qPCR, quantitative polymerase chain reaction; S100β, S100 calcium-binding protein β; SGZ, subgranular zone; snRNA-seq, single nucleus RNA sequencing; Sox1, SRY-box transcription factor 1; Sox2, SRY-box transcription factor 2; STMN1, Stathmin1; SVZ, subventricular zone; SZ, schizophrenia; Tbr2, T-box brain protein 2; TLE, temporal lobe epilepsy; Tuj1, neuron-specific class III β-tubulin.

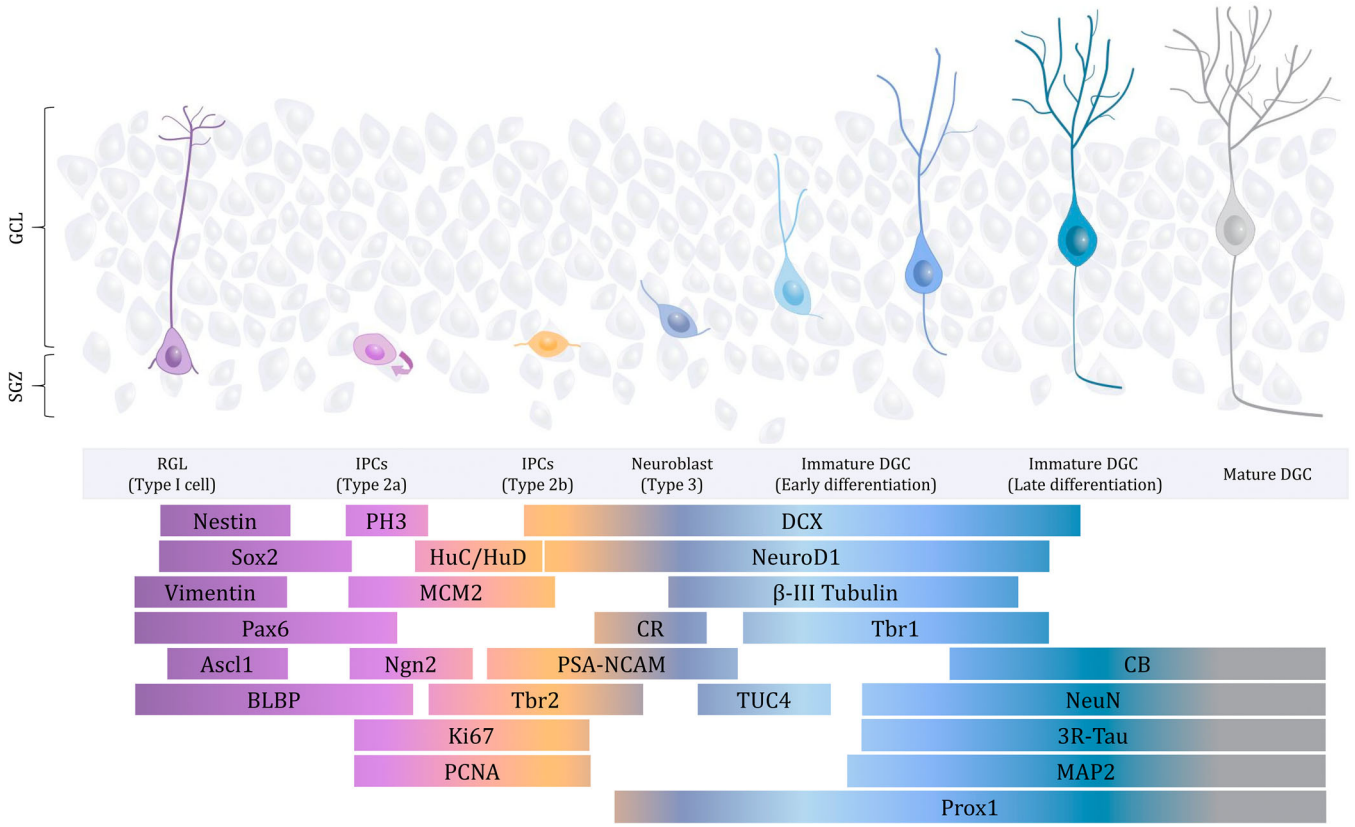

FIGURE 1 Schematic diagram showing the main stages encompassed by adult hippocampal neurogenesis (AHN). The expression of Nestin, SRY-box 2 (Sox2), Vimentin, paired box 6 (Pax6), Achaete-Scute family BHLH transcription factor 1 (Ascl1), brain lipid-binding protein (BLBP), phospho-histone 3 (PH3), human neuronal proteins C and D (HuC/D), minichromosome maintenance protein 2 (MCM2), neurogenin 2 (Ngn2), T-box brain protein 2 (Tbr2), Ki67, proliferating cell nuclear antigen (PCNA), doublecortin (DCX), neurogenic differentiation 1 (NeuroD1), β-III tubulin, calretinin (CR), polysialic acid-neural cell adhesion molecule (PSA-NCAM), prospero homeobox 1 (Prox1), T-box brain protein 1 (Tbr1), turned on after division/ulip/CRMP-4 (TUC-4), calbindin (CB), neuronal nuclei (NeuN), three-repeated tau (3RTau), and microtubule-associated protein 2 (MAP-2) is shown. DGC, dentate granule cell; GCL, granule cell layer; IPCs, intermediate progenitor cells; RGL, radial glia-like; SGZ, subgranular zone

Indeed, an exhaustive revision of the literature available reveals that tissue processing methodologies differed markedly across the studies (see Table 2). Moreover, several articles do not disclose the criteria used to validate antibodies signal on human tissue, tissue fixation protocols, detailed antigen retrieval procedures, cell counting methods, and so forth. In this regard, studies by our group quantitatively demonstrate that the fixation time, type of fixative, tissue pre-treatment, and IHC protocols dramatically limit the extent to which AHN markers are visible in the human brain (Flor-Garcia et al., 2020; Moreno-Jimenez et al., 2019; Terreros-Roncal et al., 2021), as will be further discussed throughout this review.

3 | CRITICAL STEPS TO STUDY HUMAN AHN BY IHC

3.1 | Tissue fixation

Our studies (Flor-Garcia et al., 2020; Moreno-Jimenez et al., 2019; Terreros-Roncal et al., 2021) demonstrate that prolonged fixation impedes the visualization of numerous AHN markers in the human hippocampus. Most of the antibodies used to detect these markers show optimal performance in samples fixed for ≤24 h in 4% freshly prepared PFA at 4°C (Moreno-Jimenez et al., 2019). The use of samples fixed for such short periods allows reconstruction of the main stages encompassed by human AHN, thereby enabling visualization of mature and immature neurons at distinct stages of differentiation (Flor-Garcia et al., 2020; Moreno-Jimenez et al., 2019, 2021; Terreros-Roncal et al., 2021), proliferative cells (Terreros-Roncal et al., 2021), and NSCs (Terreros-Roncal et al., 2021) in the adult human DG until at least the ninth decade of life.

To determine whether the performance of antibodies used to detect AHN markers on human brain tissue depends on the duration of tissue fixation, we obtained the whole hippocampus from several neurologically healthy control subjects (61–87 years of age). Subsequently, we divided these hippocampi into several fragments. Each fragment was fixed for a different period (namely, 1, 2, 6, 12, 24, or 48 h) in 4% freshly prepared PFA at 4°C. We next compared, for each subject, the numbers of DCX^+ and $PSA\text{-}NCAM^+$ immature neurons that were detected upon distinct fixation times (extended data fig. S2 of Moreno-Jimenez et al., 2019). One hour of fixation rendered excessively fragile samples, which also showed diminished signal intensity.

Conversely, fixation times between 2 and 12 h increased tissue robustness and allowed smooth vibratome tissue sectioning and the unambiguous observation of DCX^+ and PSA-$NCAM^+$ immature neurons. The specific signal detected in these samples was accompanied by very low background intensity. Importantly, no tissue pretreatment was needed to detect DCX^+ or PSA-$NCAM^+$ DGCs in samples fixed up to 12 h. Conversely, prolonged fixation (≥24 h) increased background intensity and masked antibody-specific signal, thereby impeding the detection of positive cells. The antigen masking caused by moderate fixation times (24–48 h) was easily reversed by applying mild antigen retrieval, sodium borohydride ($NaBH_4$) incubation, and autofluorescence elimination, as will be discussed in the next sections of this review. The optimized protocols developed by our group (Flor-Garcia et al., 2020) demonstrate the importance of the mildness of the antigen retrieval step. Despite the public availability of these protocols and data, high-intensity antigen retrieval protocols were applied in recent studies, thereby leading to the observation of an unspecific DCX signal (Franjic et al., 2022; Sorrells et al., 2021) (Table 2), as our own experiments predicted (fig. 4C in Flor-Garcia et al., 2020).

3.2 | Postmortem delay

The postmortem delay (PMD), also referred to as the postmortem interval or the delay to fixation, can be defined as the time elapsed between *exitus* and sample immersion in fixative. It should not be confounded with the fixation time (namely the time during which a sample is immersed in a fixative). Despite legal issues that unavoidably lengthen the PMD, several studies recommend the use of samples with the shortest PMD possible (de Ruiter, 1983; Eymin et al., 1993; Robinson et al., 2016; Sorensen, 1984). In general terms, proteins and ribonucleic acid (RNA) may be sensitive to postmortem degradation (Perrett et al., 1988). In fact, several authors (Kempermann et al., 2018; Lucassen, Fitzsimons, et al., 2020; Lucassen, Toni, et al., 2020) pointed to prolonged PMDs as the cause for the putative absence of AHN markers in the human DG reported by Sorrells et al. (2018).

However, subsequent research revealed that, although certain proteins may show particularly rapid postmortem degradation (Boekhoorn et al., 2006; Sorensen, 1984; Terstege et al., 2022), especially in certain regions of the brain (Siew et al., 2004), the immunodetection of most proteins and enzymes is moderately resistant to this phenomenon (Blair et al., 2016; Ritchie et al., 1986; Schut et al., 2017; Wang et al., 2000). For instance, although NR2A and NR2B subunits appear to be rapidly degraded after death (Wang et al., 2000), most subunits of N-methyl-D-aspartate (NMDA) and α-amino-3-hydroxy-5-methyl-4-isoxazolepropionic acid (AMPA)-type glutamate receptors are stable at ~18 h PMD. Studies performed by Boekhoorn et al. (2006) and Terstege et al. (2022) suggested enhanced susceptibility of DCX to postmortem degradation. These authors observed that, in rat samples with artificially induced prolonged PMDs (≥8 h), DCX staining disappears from the dendrites and is restricted to the soma and nucleus of immature DGCs. Terstege et al. reported that this phenomenon is accentuated in aged animals (Terstege et al., 2022). DCX is detected in the human DG at prolonged PMD intervals (Flor-Garcia et al., 2020; Moreno-Jimenez et al., 2019, 2021; Terreros-Roncal et al., 2021). Our quantitative and qualitative data reveal the stability not only of the number of DCX^+ immature neurons in the human DG but also dendritic staining with this marker up to at least 38 h PMD. These results suggest putative inter-species differences in either the sensitivity of DCX protein to degradation or the binding capacity of distinct anti-DCX antibodies to their respective epitopes. However, these hypotheses lack further experimental evidence.

In line with our results that moderate PMDs are compatible with the study of most AHN markers in the human brain using IHC, recent work performed on 556 postmortem human brains (6–279 h PMD) showed no significant correlation between brain pH, a widely used tissue quality indicator, and the PMD (Robinson et al., 2016). Another study (Blair et al., 2016) elegantly analyzed the intra-individual effects of artificially increasing PMDs. Those authors reported unchanged immunostaining profiles for most of the proteins studied after ≥50 h PMD, although degradation patterns were observed for several proteins by means of western blot (Blair et al., 2016). These carefully controlled experiments question the generalized notion that extended PMD is detrimental per se for the study of the human brain using IHC. Nevertheless, the results by Boekhoorn et al. (2006) and others (Terstege et al., 2022), together with the fact that the sensitivity of a particular protein to postmortem degradation cannot be predicted, indicate that performing adequate controls for each protein of interest and reporting individual PMDs should be mandatory in research protocols or scientific studies. Moreover, the use of materials with the shortest PMD possible is recommended when studying novel or putatively labile molecules (Robinson et al., 2016), and when setting up and validating new methodologies, such as single-cell (sc) or single-nucleus (sn) RNA-seq (Kalinina & Lagace, 2022).

3.3 | Autofluorescence elimination

The aged human brain is particularly enriched in a lipid pigment named lipofuscin (Glees & Hasan, 1976). Neurons accumulating lipofuscin show a characteristic granular morphology that has been described under transmitted light, fluorescence, and electron microscopy (Glees & Hasan, 1976). The presence of lipofuscin granules in the human brain increases with age but starts to be observed during the first decade of life (Goyal, 1982). Indeed, immature and newly generated neurons exhibit less lipofuscin than their developmentally generated counterparts (Ernst et al., 2014; Roeder et al., 2022; Spalding et al., 2013).

In addition to the presence of abundant lipofuscin granules, brain tissue shows a great amount of primary background fluorescence (autofluorescence). It has been known for several decades that the autofluorescence of cell and tissue components depends on the

fixative used and fixation time, as well as on excitation wavelength (Del Castillo et al., 1989). In particular, aldehyde fixation causes higher autofluorescence than methanol or ethanol/acetic acid (Del Castillo et al., 1989). Autofluorescence related to aldehyde fixation is attributed to the formation of Schiff's bases between amines released upon cell death and the aldehydes present in the fixative solution (Willingham, 1983). Importantly, Schiff's bases show high autofluorescence capacity. In fact, the intense autofluorescence observed in the human brain compromises the visualization and signal specificity of numerous antibodies. Several strategies have been used to decrease or eliminate autofluorescence in this tissue. Clancy et al. showed that a 30-min immersion of free-floating brain tissue sections in a sodium borohydride ($NaBH_4$, 0.1%) solution reduces background fluorescence by ~30% (Clancy & Cauller, 1998), as this compound neutralizes Schiff's bases by reducing the amine-aldehyde compounds into their corresponding non-fluorescent salts (Clancy & Cauller, 1998; Willingham, 1983). We (Flor-Garcia et al., 2020; Moreno-Jimenez et al., 2019; Terreros-Roncal et al., 2021) and others (Boldrini et al., 2018; Boldrini et al., 2009) have successfully subjected such samples to $NaBH_4$ incubation when studying human AHN. In particular, our data revealed that a 30-min incubation with a 0.5% solution of $NaBH_4$ reduces background autofluorescence by ~40% (fig. 4E and F in Flor-Garcia et al., 2020) and is therefore optimal for the visualization of several AHN markers in the human DG (Flor-Garcia et al., 2020; Moreno-Jimenez et al., 2019; Terreros-Roncal et al., 2021).

Other reagents, such as Sudan black (Baschong et al., 2001; Kajimura et al., 2016), are useful to remove autofluorescence from human brain tissue. In particular, the use of commercial solutions of Sudan Black (such as the Autofluorescence Eliminator reagent [EMD Millipore]) reduces background and lipofuscin granule intensity in human DG samples, thereby facilitating the identification of AHN markers (fig. 5 in Flor-Garcia et al., 2020). Other strategies, such as the use of LED lamps to quench fluorophores, have been assayed to eliminate autofluorescence in predominantly non-mitotic tissues such as the human brain (Sun et al., 2017).

In our hands, the most effective strategy to remove autofluorescence from aldehyde-fixed human brain samples combines a 30-min incubation with a 0.5% solution of $NaBH_4$ before IHC with a brief (5-min) incubation with a commercial solution of Sudan Black (Autofluorescence Eliminator reagent [EMD Millipore]) at the end of the IHC protocol (Flor-Garcia et al., 2020; Moreno-Jimenez et al., 2019, 2021; Terreros-Roncal et al., 2021). Importantly, none of these steps should be confounded with antigen-retrieval protocols, aimed at unmasking antibody-specific signal and which are further discussed below.

3.4 | Antigen retrieval

Although some epitopes are unaffected by the PMD (Bowers et al., 2003), epitope masking might unavoidably occur after prolonged aldehyde fixation. This process prevents antibodies from detecting and binding the antigens they have been raised against. To unmask epitopes that are especially sensitive to the fixation process, distinct antigen retrieval protocols can be applied to increase the specificity of the signal detected (Smith & Lippa, 1995). We and others have observed that antigen retrieval protocols are necessary to detect only certain antigens and under specific fixation conditions (Flor-Garcia et al., 2020; Moreno-Jimenez et al., 2019, 2021; Terreros-Roncal et al., 2021, 2022a, 2022b). In this regard, the detection of DCX in samples fixed for ≤12 h does not require the application of antigen retrieval protocols (Moreno-Jimenez et al., 2019). In contrast, samples fixed for 24–48 h, need to be subjected to a mild heat-mediated citrate buffer antigen retrieval protocol (HC-AR) (Moreno-Jimenez et al., 2019). The mildness of the latter step is crucial to increase the intensity of the specific signal without affecting that of the background (Flor-Garcia et al., 2020). Conversely, our studies show that the application of a harsh antigen retrieval approach cause the appearance of an unspecific antibody signal (Flor-Garcia et al., 2020). We have optimized an antigen retrieval protocol to achieve high-quality performance on human DG samples (Flor-Garcia et al., 2020; Moreno-Jimenez et al., 2019; Terreros-Roncal et al., 2021). This protocol consists of exposing brain samples immersed in a commercial citrate buffer-based solution to short and strictly controlled microwave radiation cycles, followed by a subsequent 20-min incubation in a water bath. Given that aggressive antigen retrieval may lead to lack of signal specificity, our results show that finely adjusting the characteristics of antigen retrieval protocols is an essential step required to perform rigorous AHN studies (fig. 4C in Flor-Garcia et al., 2020).

Other authors have reported that, depending on the duration of tissue fixation, distinct antigen retrieval conditions are optimal for the detection of particular epitopes. In general, long fixation times require high-intensity antigen retrieval (increased heating duration and/or use of lower pH values [Taylor et al., 1994]). For instance, it has been proposed that the detection of the proliferation marker Ki-67 is optimal when antigen retrieval is performed at low pH (Shi et al., 1995), whereas standard pH 6.0 is suboptimal for samples fixed for longer than 24 h (Munakata & Hendricks, 1993). In fact, Boekhoorn et al. (2006) compared the adequacy of antigen retrieval under distinct pH conditions, namely pH 1.0 (0.1 M HCL), pH 3.0 (0.01 M citrate buffer), pH 6.0 (0.01 M citrate buffer) and pH 9.0 (0.01 M Tris), to detect Ki-67^+ signal in the human DG. Those authors concluded that the lowest pH renders the highest quality signal on human adult hippocampal tissue. Similar systematic studies are, therefore, needed to optimize antigen retrieval protocols for each antibody intended to be used on human brain samples.

3.5 | The immunohistochemistry protocol

3.5.1 | Antibody signal validation

The validation of primary and secondary antibodies is essential to assess any biological process using IHC. Moreover, given discrepant

results reported in the literature, unambiguous signal validation gains further relevance in the context of AHN studies. Although an antibody is theoretically designed to target a protein of interest in a particular species, some antibodies produce unspecific staining, high background, or artifactual detection of other proteins (Flor-Garcia et al., 2020). Moreover, determining whether an observed signal is indeed specific is not straightforward. Despite inter-species differences, a general recommendation to validate a new antibody in a given species is to compare the signal obtained with that described in rodents (whenever this information is available). In this regard, the subcellular distribution of the signal observed should be, a priori, similar in both species (for instance, a microtubule-associated protein is expected to label cytoplasmic structures). Also, the same cell types are expected to be either positive or negative for that marker in both species. In this respect, morphological criteria can be used to identify cell types. However, evaluation of the co-expression of other markers that have been validated previously is advised whenever possible (Flor-Garcia et al., 2020; Moreno-Jimenez et al., 2021; Terreros-Roncal et al., 2021). If unexpected cell types appear to show positive staining, further validation with alternative methods (see below) might be required. In particular, in the case of AHN makers, widespread signal is not expected to be observed in non-neurogenic regions of the brain, although there might be exceptions. In this regard, observations of staining with anti-DCX antibodies in non-neurogenic regions have been used to refute the occurrence of human AHN (Alvarez-Buylla et al., 2022; Sorrells et al., 2021). This assumption overlooks two important considerations: first, the existence of DCX^+ neurons in non-neurogenic regions of the mouse brain is compatible with the occurrence of rodent AHN and there is no evidence supporting the opposite in humans. Second, a recent study revealed that the DCX^+ signal observed in the macaque cortex is not only unspecific but also artifactual (Liu et al., 2020). This finding thus calls for caution when interpreting DCX^+ signal in non-neurogenic regions of the primate brain (Terreros-Roncal et al., 2022b).

To assess the specificity of a given antibody, distinct strategies, such as the use of synthetic blocking peptides that mimic the antigen recognition domain by antibodies (Liu et al., 2020; Moreno-Jimenez et al., 2019), can be tested. For instance, the pre-adsorption of an anti-DCX antibody with a specific blocking peptide causes the disappearance of the DCX^+ signal by both dot-blot and IHC (Moreno-Jimenez et al., 2019), thereby confirming the authenticity of the DCX signal detected in the human DG. Strikingly, the incubation of anti-DCX antibodies with hippocampal extracts causes the DCX^+ signal to disappear in macaque cortices but not in the hippocampi of this animal (Liu et al., 2020). These results question the specificity of certain anti-DCX antibodies used in previous studies (Sorrells et al., 2018), as they might detect other proteins that potentially share structural properties with DCX in some regions of the primate brain (Liu et al., 2020).

It is also important to note that not all the commercially available antibodies raised against a given protein render specific signal even under ideal sample processing conditions (Flor-Garcia et al., 2020). To further validate DCX staining in the human DG, we quantitatively compared the performance of various anti-DCX antibodies raised against distinct domains of the protein. As shown in Moreno-Jimenez et al. (2019), the quality of the signal, the signal/background ratio, and the working concentrations differed among the distinct commercial antibodies tested. However, all of them rendered comparable numbers of DCX^+ immature neurons (Moreno-Jimenez et al., 2019). This finding thus supports the suitability of these antibodies to specifically detect DCX in the human DG. As previously mentioned, none of the nine commercially available antibodies we tested were able to detect DCX^+ cells in human hippocampal samples fixed for 6 months in formalin (Flor-Garcia et al., 2020; Moreno-Jimenez et al., 2019). Importantly, the lack of DCX signal caused by excessive fixation was observed not only in adult samples but also in tissue obtained from juvenile and infantile subjects (Figure 2), in which the occurrence of neurogenesis has not been disputed to date.

3.5.2 | IHC buffer

Additionally, the optimal detection of certain antigens might require particular IHC conditions. In this regard, the choice of the detergent present in wash and incubation buffers is frequently overlooked in the design of antibody validation protocols. Our data show that one of the most used detergents, namely Triton X-100, is suboptimal for the detection of NSC markers such as Nestin in the adult human hippocampus (Terreros-Roncal et al., 2021). Triton X-100 replacement by a milder detergent, such as saponin, enables the detection of cells positive for Nestin in this structure (Terreros-Roncal et al., 2021). The combination of Nestin with astrocyte markers such as S100β has revealed the phenotypic NSC properties of these cells in the human hippocampus (Terreros-Roncal et al., 2021). NSCs express Nestin, Vimentin, Sox2 and GFAP but lack S100β. Moreover, these cells show specific morphological properties (such as their main location at the SGZ and the presence of long, distally-branched processes that transverse the GCL) (Terreros-Roncal et al., 2021, 2022a, 2022b). Although we have found that saponin negatively impacts the detection of other AHN markers, the signal intensity or signal/background ratio may experience slight variations with respect to the use of Triton X-100. In this regard, signal characteristics should be tightly monitored when setting up the use of new antibodies.

3.6 | CELL COUNT METHODS

The number of cells positive for AHN markers reported in distinct studies shows apparently dissimilar orders of magnitude, which can be attributed to a variety of technical reasons. In this respect, although unbiased stereological methods were applied in several of these studies (Boldrini et al., 2018; Flor-Garcia et al., 2020; Knoth et al., 2010; Moreno-Jimenez et al., 2019; Terreros-Roncal et al., 2021; Tobin et al., 2019), the strategies applied to determine cell numbers were not coincident (see Table 2).

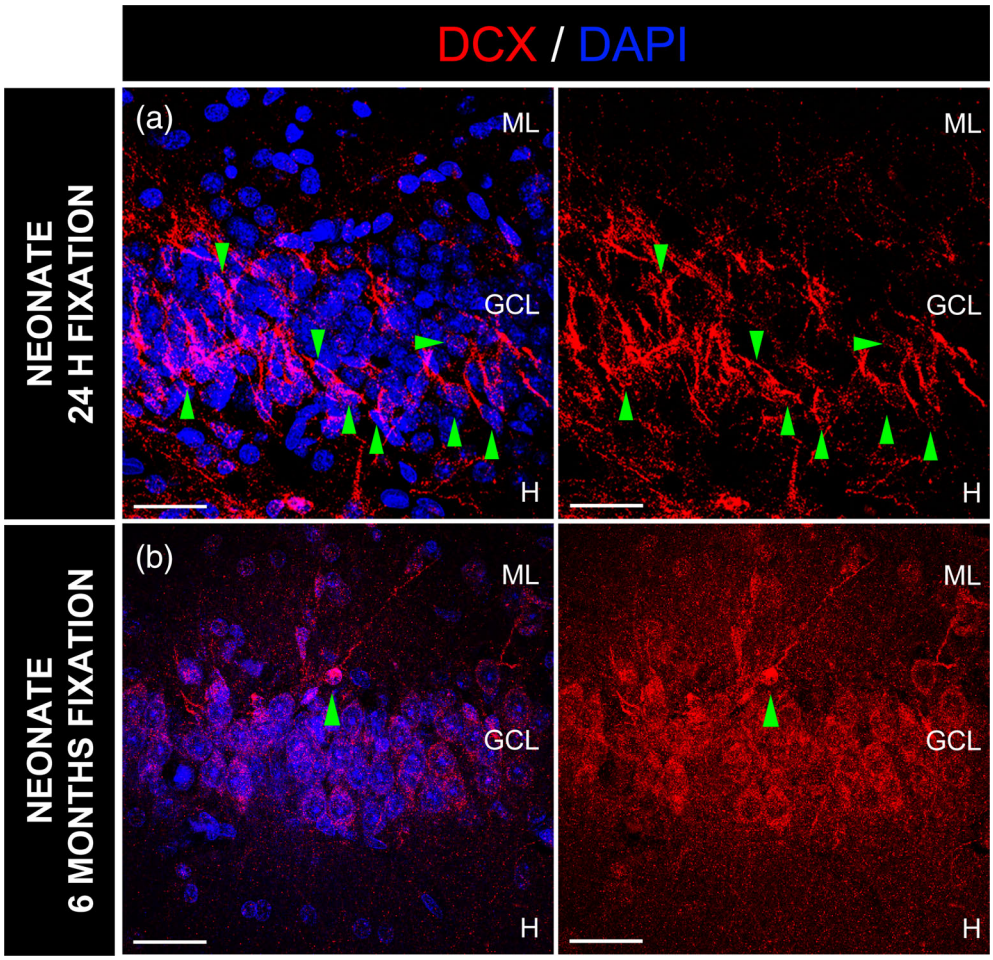

FIGURE 2 Immature neurons in the infantile human hippocampus. (a) Neonate human hippocampus upon 24 h of sample fixation in 4% freshly prepared paraformaldehyde. The presence of abundant immature neurons is detected. (b) Neonate human hippocampus upon 6 months of fixation. The presence of immature neurons is no longer detected in this sample. White scale bar: 50 μm. DAPI, 4′,6-diamidino-2-phenylindole; DCX, doublecortin; GCL, granule cell layer; Green triangles, immature neurons; H, hilus; ML, molecular layer

The use of stereology frequently involves normalization of the number of cells counted by the reference volume/area (namely the volume/area of the structure in which cells were counted). Therefore, the choice of such a reference structure is the first source of variability. Some studies divided the number of cells counted by the length of the SGZ/GCL boundary or by that length multiplied by the thickness of the section, whereas in other studies, such as ours (Flor-Garcia et al., 2020; Moreno-Jimenez et al., 2019; Terreros-Roncal et al., 2021), the number of cells counted was divided by the volume of the GCL. Therefore, the resulting cell densities calculated in these studies have, indeed, distinct orders of magnitude and units (number of cells/mm or cells/mm^2 vs. number of cells/mm^3).

Cell counts can be performed using automated cell detection software or can be done manually, which further increases putative sources of variability between studies. Some authors applied semi-automatic systems such as Stereoinvestigator to calculate cell numbers, as well as to detect the reference volume/length (Boldrini et al., 2018; Tobin et al., 2019). Conversely, we performed an unbiased random sampling of the tissue by acquiring several individual stacks of images per subject under a confocal microscope, which was followed by manual cell counts (Flor-Garcia et al., 2020; Moreno-Jimenez et al., 2019; Terreros-Roncal et al., 2021). Automatic versus manual cell count systems may use distinct criteria to assign a given cell the attribute of "positive" for a certain marker, Moreover, these systems may show variable signal detection thresholds or may present distinct capacity to discriminate signal versus background, among other factors, thereby accounting for great variations in the number of cells detected.

Moreover, not only does the microscopy equipment used (confocal, conventional, or epifluorescence microscopes) differ between studies but so does the unbiased stereological method applied to estimate cell densities. Several studies used optical dissector and fractionator methods (Boldrini et al., 2018; Tobin et al., 2019), in which a device coupled to an optical microscope goes through the entire thickness of the tissue to detect positive cells. Conversely, other groups, such as ours, used the physical dissector method coupled to confocal microscopy for cell count purposes (Llorens-Martin, Torres-Aleman, & Trejo, 2006). In the latter method, extremely thin sections are obtained under a confocal microscope, thereby allowing for accurate Z-axis resolution and furthering the precision of cell counts (Llorens-Martin et al., 2006).

A very small number of human AHN studies have reported total numbers of cells in the entire DG (Boldrini et al., 2018; Tobin et al., 2019), for which previous determination of the DG total volume is required but is not always possible. To circumvent this difficulty, other studies, such as ours (Flor-Garcia et al., 2020; Moreno-Jimenez et al., 2019; Terreros-Roncal et al., 2021), reported relative

(normalized) cell densities. Therefore, a direct comparison of normalized versus absolute numbers of cells is not possible. Similarly, two studies (Boldrini et al., 2018; Tobin et al., 2019) examined the whole rostro-caudal extent of the human DG, whereas only the posterior pole of the anterior hippocampus was examined in Moreno-Jimenez et al. (2019) and Terreros-Roncal et al. (2021). Consequently, differences in the precise anatomical regions examined may add further disparity to the number of cells reported.

In light of the variety of methodological approaches used to perform cell counts in the available literature (see Table 2), data showing distinct orders of magnitude or units should not be considered contradictory a priori but rather interpreted as being calculated and reported in a dissimilar manner.

4 | COMPLEMENTARY METHODOLOGIES TO THE USE OF IHC

Although most studies addressing the occurrence of human AHN in vivo are based on the use of IHC (see Table 2), several studies explored alternative methodological approaches, as discussed below.

In 2007, the use of functional magnetic spectroscopy by Maletic-Savatic's group allowed the detection of human and murine hippocampal NSCs in vivo (Manganas et al., 2007). Further research by that group revealed putative metabolites that could account for that specific signal (Kandel et al., 2022). The approach proposed by Maletic-Savatic's group paved the way for the subsequent development of strategies aimed at noninvasively detecting AHN levels, such as the design of novel ligands and enhanced detection methods for positron emission tomography (PET) brain imaging (Tamura et al., 2016). The potential for further optimization of such noninvasive methodologies lies in their capacity not only to monitor the rate of AHN in living subjects but also to potentially allow the correlation of AHN with, for instance, cognitive scores. Such correlative analyses might be relevant to determine the role played by newly generated neurons in human behavior. Alternatively, some authors have proposed an in vitro approach to correlate proxies for human adult neurogenesis and, for example, cognitive scores (Du Preez, Lefevre-Arbogast, Gonzalez-Dominguez, et al., 2022; Du Preez, Lefevre-Arbogast, Houghton, et al., 2022).

Several years ago, Frisen's group developed a ground-breaking methodology, based on the measurement of C^{14} incorporation into the adult brain, which allowed them to demonstrate the addition of new neurons to certain brain regions such as the hippocampus and the striatum (Ernst et al., 2014; Spalding et al., 2013). They corroborated their findings by IHC and lipofuscin quantification, which revealed the presence of newborn immature neurons in these structures. Moreover, using mathematical modeling, they determined that 700 new neurons are added daily to the human DG.

In recent years, scRNAseq/snRNAseq have been used to reconstruct cellular trajectories in various animal species. Regarding human studies, strong discrepancies are found in the literature, even upon the re-analysis of published datasets (Ayhan et al., 2021; Franjic et al., 2022; Habib et al., 2017; Sorrells et al., 2021). Such discrepancies might be partially related to technical dissimilarities between studies (reviewed in Kalinina and Lagace, 2022). In this regard, dramatic variations in sample characteristics (including the PMD), tissue dissection, cell/nuclei isolation and purification, and result analysis are found in the literature (Kalinina & Lagace, 2022). Of note, Ayhan et al. (2021) used biopsy samples with ~12 min PMD, which likely rendered high-quality transcriptomes and which sharply contrast with the prolonged 9–12 h PMD used in Franjic et al. (2022).

One of the first key steps in sc- and sn-RNAseq protocols is the generation of high-quality single-cell suspensions. sc-RNAseq has been shown to outperform sn-RNAseq as it captures more transcripts per cell (Ding et al., 2020; Habib et al., 2017). Most studies addressing human AHN have used the "Frankenstein" method for cell suspension preparations (Ayhan et al., 2021; Habib et al., 2017; Tran et al., 2021). Conversely, Franjic et al. used sucrose gradient centrifugation to isolate nuclei (Franjic et al., 2022). The number of cells/nuclei analyzed in distinct scRNAseq/snRNAseq human AHN studies presents remarkable variability (14,963 hippocampal cells obtained from 4 male non-diseased donors [40–65 years] and subjected to Drop-seq and DroNc-seq were analyzed by means of Seurat in Habib et al., 2017; 10,268 cells obtained from 3 male neurotypical donors [40–69 years] were analyzed by means of 10× Genomics, Bioconductor, and MAGMA in Tran et al., 2021; 109,208 cells isolated from 5 male and female patients [24–60 years] with epilepsy were subjected to 10× Genomics, Seurat, GO, and MAST in Ayhan et al., 2021; 32,067 DG cells obtained from 6 male and female clinically unremarkable donors [~52 years] were subjected to 10× Genomics and analyzed by means of Seurat, Velocyto, and scVelo in Franjic et al., 2022; 22,119 cells obtained from 4 male and female subjects [67–92 years] were subjected to 10× Genomics sc-RNAseq and sc-ATAC-seq and analyzed by means of Seurat, Signac, and Cell Ranger in Wang et al., 2022; and 151,701 nuclei obtained from 38 male and female subjects [20 gw–92 years] were subjected to Drop-seq and SPLiT-seq and analyzed by means of Seurat, supervised machine learning approaches in Zhou et al., 2022). Noise control strategies and cell exclusion criteria also varied dramatically between these studies.

The aforementioned methodological variability, together with a notable diversity in the depth of analysis of these studies, may account for their distinct resolution capacity to identify various cell populations, especially those that are present in low abundance, such as NSCs. It should be noted that, according to our own quantitative data, it would be necessary to analyze 1,000,000 DGCs to detect a cluster of 200 NSCs in the human DG (Terreros-Roncal et al., 2021). In this regard, Franjic et al. failed to identify NSCs in the DG of three adult human subjects (Franjic et al., 2022). Conversely, Ayhan et al. (2021), Habib et al. (2017), Wang et al. (2022), and Zhou et al. (2022) robustly identified a quantitatively modest but detectable cluster with neural progenitor characteristics in the adult human DG. Moreover, the latter publication provided the first reconstruction of the entire primate AHN trajectory by means of snRNA-seq, thereby identifying a maturation continuum from quiescent and active NSCs to proliferative cells, early and late immature DGCs, and mature DGCs in human

TABLE 3 Comparison between methodologies used in distinct original publications undertaking single-cell (sc)- and single-nucleus (sn)-RNAseq studies on primates

Reference	Age	Sex	Dissociation	PMD (h)	Platform	Analysis	AHN trajectory	Cell number
(Habib et al., 2017)	40–65 years (human)	4M	"Frankenstein" (FACS)	~12.4 h	Drop-seq, DroNc-seq	Seurat	Yes	14,963
(Tran et al., 2021)	40.08–54.43 years (human)	3M	"Frankenstein" (FACS)	21.5–38 h	10× Genomics	Bioconductor, MAGMA	No	10,268
(Ayhan et al., 2021)	24–60 years (human)	2M/3F	"Frankenstein" (FACS)	0 h	10× Genomics	Seurat, GO, MAST	Yes	129,908
(Franjic et al., 2022)	DG: 44–48 years (human) 8.6–14.2 years (macaque)	Human: 3M (DG) Macaque: 3F	Sucrose gradient centrifugation	Human: 17–21 h (DG) Macaque: ≤1 h	10× Genomics. cDNA was amplified for 14 cycles. Nuclei with >10% mitochondrial content were excluded	Seurat, Velocyto, scVelo. Clustering with FindClusters	No	32,067 (human) and 19,803 (macaque) DG cells
(Hao et al., 2022)	4–15 years (macaque)	6M/2F	Specifically developed scRNA-seq pipeline	0 h	10× Genomics Chromium sc Kit v3	Cell Ranger Scrublet, SCANPY, SCENIC, pySCENIC, Cytoscape, UMAP, Louvain, SCCAF, Seurat, MAST, RNA velocyto and scVelo	Yes	207,785
(Wang et al., 2022)	67–92 years (human) 0–23 years (macaque)	Human: 3M/1F Macaque: 11M/2F	Tissue minced into <5 mm pieces and homogenized. Density gradient centrifugation	Human: 5–20.5 h Macaque: 0 h	10× Genomics Chromium sc Kit v3 and Chromium Single Cell ATAC v1.0	Seurat, Signac, Cell Ranger. Clustering with FindNeighbors and FindClusters	Yes	22,119 (human) and 132,524 (macaque)
(Zhou et al., 2022)	20 gw–92 years (human)	Human: 23M/15F	Modified SPLiT-seq approach for nuclei isolation and snRNA-seq. Snap-frozen tissue	Human: 2.3–44 h	Drop-seq, SPLiT-seq. Nuclei with >5% UMIs mapped to mitochondrial genes were excluded	Seurat (v.3.6), Supervised learning approach (modified multinomial machine learning (implemented in the LogisticRegression function in scikit-learn60 in Python v3.7) was applied. Multi-class random forest classifier (v4.6.14). cVI40	Yes	Human: 0–2 years, $n = 4$: 15,434 nuclei; 3–6 years, $n = 4$: 24,607 nuclei; 13–18 years, $n = 4$; 16,310 nuclei; 40–60 years, $n = 5$: 29,832 nuclei; 86–92 years, $n = 5$: 16,055 nuclei; AD, 73–88 years, $n = 8$: 27,508 nuclei;

TABLE 3 (Continued)

Reference	Age	Sex	Dissociation	PMD (h)	Platform	Analysis	AHN trajectory	Cell number
						(v0.6.8) in Python (v3.7). Monocle41 (v2.8). ClueGO (v.2.5.5) plug-in64 in Cytoscape65 (v3.7.2). CellPhoneDB42 tool (v2.1.4)		and matched controls, 73–88 years, $n = 8$: 21,955 nuclei

Note: This table was constructed after performing a manual search of studies that included the following terms (and their combination thereof) in the PubMed database: "Adult hippocampal neurogenesis," "Human," "sc-RNAseq," and "sn-RNAseq." Studies not focused on the human hippocampal region or that examined only other species were manually excluded.
Abbreviations: cDNA, complementary deoxyribonucleic acid; F, female; FACS, fluorescence-activated cell sorting; M, male.

beings and macaques (Wang et al., 2022), as did another recent publication in the latter species (Hao et al., 2022). The study by Zhou et al. (2022) further confirmed the proliferative capacity of the human DG by showing in vitro EdU (5-ethynyl-2′-deoxyuridine) incorporation into this structure. Moreover, proliferative cells expressed neuronal markers after several weeks. The results of these studies thus raise important caveats about the negative results reported in other studies.

Despite the potential usefulness of sc- and sn-RNAseq to reconstruct entire cellular trajectories, important technical aspects, such as the impact of distinct cell isolation methods, the PMD, and other factors, remain unsolved. Moreover, the lack of consensus validation criteria, variations in threshold and clustering strategies, together with putative artifacts derived from tissue processing (Marsh et al., 2022), may underpin the existing controversy between sc/sn-RNAseq studies. Additionally, important numerical considerations, such as the required minimum number of high-quality cells/nuclei required for any intended analysis, need to be carefully examined to adequately interpret results, especially in the context of negative results. Table 3 summarizes the most important methodological aspects that differ between various original publications that aimed to address AHN in primates using sc- and sn-RNAseq.

5 | FINAL CONSIDERATIONS

The publication of a study in 2018 proposing the absence of AHN markers in the adult human hippocampus (Sorrells et al., 2018) gave rise to so-called *controversy* in the field. This *controversy* revolved around whether cells positive for AHN markers were present in the human DG. We experimentally demonstrated that certain tissue processing methodologies (such as prolonged fixation, or absence/inadequacy of antigen retrieval protocols) are incompatible with the observation of well-validated AHN markers in this structure. Our studies revealed that NSCs, neuroblasts, and immature neurons are present in the adult human DG until at least the ninth decade of life (Flor-Garcia et al., 2020; Moreno-Jimenez et al., 2019; Terreros-Roncal et al., 2021).

Once this fundamental aspect of the original *controversy* had been resolved, public debate has been diversified into other secondary aspects, mostly unrelated to the original topic, and not supported by experimental evidence either, as previously discussed (Terreros-Roncal et al., 2022b). Our strict control experiments reveal that overlooking crucial methodological aspects may potentially have (temporary) consequences for any field of research. Whether slight methodological variations have a similar impact on the study of other processes putatively occurring in the adult human brain (or on the identification of novel neurogenic niches) remains to be fully elucidated. Nevertheless, our results highlight the need for rigorous reporting of methodological details in human studies to facilitate reproducibility between laboratories.

AHN is one of the most extraordinary reserves of plasticity in the adult mammalian brain. We are confident that our systematic studies addressing fundamental biological questions will positively contribute to the overall advance of the AHN field and will enhance our understanding of the mechanisms governing the generation of new neurons during both physiological and pathological aging throughout human life.

ACKNOWLEDGMENTS

This study was supported by the following: The European Research Council (ERC) (ERC-CoG-2020-101001916); the Spanish Ministry of Economy and Competitiveness (PID2020-113007RB-I00, SAF-2017-82185-R, and RYC-2015-171899); The Alzheimer's Association (2015-NIRG-340709, AARG-17-528125, and AARG-17-528125-RAPID), The Association for Frontotemporal Degeneration (2016 Basic Science Pilot Grant Award); and the Center for Networked Biomedical Research on Neurodegenerative Diseases (CIBERNED, Spain). Institutional grants from the Fundación Ramón Areces and Banco de Santander to the CBMSO are also acknowledged. The salary of B. M-V. was supported by postdoctoral fellowships awarded by the Consejo Nacional de Ciencia y Tecnología (CONACYT) of the Mexican Government (Reference CVU Number: 385084) and the Secretaria de Educación, Ciencia Tecnología e Innovación (SECTEI) of the Regional Government of Ciudad de México (CDMX) (SECTEI/159/2021). The salary of J.T-R was suppoerted by a FPI-UAM fellowship. The salary of E. P. M-J was supported by a Fundación Tatiana Pérez de Guzmán fellowship. The salary of M. F-G was supported by a Formación de Personal Investigador (FPI) fellowship (PRE2018-085233). The salary of M. F-G was supported by a Formación de Personal Investigador (FPI) fellowship (PRE2021-097690).

CONFLICT OF INTEREST

The authors declare no competing interest.

DATA AVAILABILITY STATEMENT

This review does not include any primary data.

ORCID

Julia Terreros-Roncal https://orcid.org/0000-0003-4247-6368
Miguel Flor-García https://orcid.org/0000-0002-6938-9689
Elena P. Moreno-Jiménez https://orcid.org/0000-0002-9865-4875
Carla B. Rodríguez-Moreno https://orcid.org/0000-0003-0738-7597
Berenice Márquez-Valadez https://orcid.org/0000-0001-7812-2284
Marta Gallardo-Caballero https://orcid.org/0000-0002-3771-0132
María Llorens-Martín https://orcid.org/0000-0001-9129-5198

REFERENCES

Akers, K. G., Martinez-Canabal, A., Restivo, L., Yiu, A. P., De Cristofaro, A., Hsiang, H. L., Wheeler, A. L., Guskjolen, A., Niibori, Y., Shoji, H., Ohira, K., Richards, B. A., Miyakawa, T., Josselyn, S. A., & Frankland, P. W. (2014). Hippocampal neurogenesis regulates forgetting during adulthood and infancy. *Science*, *344*(6184), 598–602. https://doi.org/10.1126/science.1248903

Allen, K. M., Fung, S. J., & Weickert, C. S. (2016). Cell proliferation is reduced in the hippocampus in schizophrenia. *The Australian and New Zealand Journal of Psychiatry*, *50*(5), 473–480. https://doi.org/10.1177/0004867415589793

Alpar, A., Kunzle, H., Gartner, U., Popkova, Y., Bauer, U., Grosche, J., Reichenbach, A., & Hartig, W. (2010). Slow age-dependent decline of doublecortin expression and BrdU labeling in the forebrain from lesser hedgehog tenrecs. *Brain Research*, *1330*, 9–19. https://doi.org/10.1016/j.brainres.2010.03.026

Altman, J. (1963). Autoradiographic investigation of cell proliferation in the brains of rats and cats. *Anatomical Record*, *145*, 573–591.

Alvarez-Buylla, A., Cebrian-Silla, A., Sorrells, S. F., Nascimento, M. A., Paredes, M. F., Garcia-Verdugo, J. M., Yang, Z., & Huang, E. J. (2022). Comment on "Impact of neurodegenerative diseases on human adult hippocampal neurogenesis". *Science*, *376*(6590), eabn8861. https://doi.org/10.1126/science.abn8861

Ammothumkandy, A., Ravina, K., Wolseley, V., Tartt, A. N., Yu, P. N., Corona, L., Zhang, N., Nune, G., Kalayjian, L., Mann, J. J., Rosoklija, G. B., Arango, V., Dwork, A. J., Lee, B., Smith, J. A. D., Song, D., Berger, T. W., Heck, C., Chow, R. H., … Bonaguidi, M. A. (2022). Altered adult neurogenesis and gliogenesis in patients with mesial temporal lobe epilepsy. *Nature Neuroscience*, *25*(4), 493–503. https://doi.org/10.1038/s41593-022-01044-2

Amrein, I., Becker, A. S., Engler, S., Huang, S. H., Muller, J., Slomianka, L., & Oosthuizen, M. K. (2014). Adult neurogenesis and its anatomical context in the hippocampus of three mole-rat species. *Frontiers in Neuroanatomy*, *8*(May), 39. https://doi.org/10.3389/fnana.2014.00039

Amrein, I., Dechmann, D. K., Winter, Y., & Lipp, H. P. (2007). Absent or low rate of adult neurogenesis in the hippocampus of bats (Chiroptera). *PLoS One*, *2*(5), e455. https://doi.org/10.1371/journal.pone.0000455

Amrein, I., Nosswitz, M., Slomianka, L., van Dijk, R. M., Engler, S., Klaus, F., Raineteau, O. & Azim, K. (2015). Septo-temporal distribution and lineage progression of hippocampal neurogenesis in a primate (Callithrix jacchus) in comparison to mice. *Frontiers in Neuroanatomy*, *9*, 85. https://doi.org/10.3389/fnana.2015.00085

Amrein, I., & Slomianka, L. (2010). A morphologically distinct granule cell type in the dentate gyrus of the red fox correlates with adult hippocampal neurogenesis. *Brain Research*, *1328*, 12–24. https://doi.org/10.1016/j.brainres.2010.02.075

Amrein, I., Slomianka, L., Poletaeva, I. I., Bologova, N. V., & Lipp, H. P. (2004). Marked species and age-dependent differences in cell proliferation and neurogenesis in the hippocampus of wild-living rodents. *Hippocampus*, *14*(8), 1000–1010. https://doi.org/10.1002/hipo.20018

Ayhan, F., Kulkarni, A., Berto, S., Sivaprakasam, K., Douglas, C., Lega, B. C., & Konopka, G. (2021). Resolving cellular and molecular diversity along the hippocampal anterior-to-posterior axis in humans. *Neuron*. https://doi.org/10.1016/j.neuron.2021.05.003

Barker, J. M., Wojtowicz, J. M., & Boonstra, R. (2005). Where's my dinner? Adult neurogenesis in free-living food-storing rodents. *Genes, Brain, and Behavior*, *4*(2), 89–98. https://doi.org/10.1111/j.1601-183X.2004.00097.x

Bartkowska, K., Djavadian, R. L., Taylor, J. R., & Turlejski, K. (2008). Generation recruitment and death of brain cells throughout the life cycle of *Sorex shrews* (Lipotyphla). *The European Journal of Neuroscience*, *27*(7), 1710–1721. https://doi.org/10.1111/j.1460-9568.2008.06133.x

Bartkowska, K., Turlejski, K., Grabiec, M., Ghazaryan, A., Yavruoyan, E., & Djavadian, R. L. (2010). Adult neurogenesis in the hedgehog (*Erinaceus concolor*) and mole (*Talpa europaea*). *Brain, Behavior and Evolution*, *76*(2), 128–143. https://doi.org/10.1159/000320944

Baschong, W., Suetterlin, R., & Laeng, R. H. (2001). Control of autofluorescence of archival formaldehyde-fixed, paraffin-embedded tissue in confocal laser scanning microscopy (CLSM). *The Journal of*

Histochemistry and Cytochemistry, *49*(12), 1565–1572. https://doi.org/10.1177/002215540104901210

Bayer, R., Franke, H., Ficker, C., Richter, M., Lessig, R., Buttner, A., & Weber, M. (2015). Alterations of neuronal precursor cells in stages of human adult neurogenesis in heroin addicts. *Drug and Alcohol Dependence*, *156*, 139–149. https://doi.org/10.1016/j.drugalcdep.2015.09.005

Bekiari, C., Grivas, I., Tsingotjidou, A., & Papadopoulos, G. C. (2020). Adult neurogenesis and gliogenesis in the dorsal and ventral canine hippocampus. *The Journal of Comparative Neurology*, *528*(7), 1216–1230. https://doi.org/10.1002/cne.24818

Blair, J. A., Wang, C., Hernandez, D., Siedlak, S. L., Rodgers, M. S., Achar, R. K., Fahmy, L. M., Torres, S. L., Petersen, R. B., Zhu, X., Casadesus, G., & Lee, H. G. (2016). Individual case analysis of postmortem interval time on brain tissue preservation. *PLoS One*, *11*(3), e0151615. https://doi.org/10.1371/journal.pone.0151615

Blümcke, I., Schewe, J. C., Normann, S., Brüstle, O., Schramm, J., Elger, C. E., & Wiestler, O. D. (2001). Increase of nestin-immunoreactive neural precursor cells in the dentate gyrus of pediatric patients with early-onset temporal lobe epilepsy. *Hippocampus*, *11*(3), 311–321. https://doi.org/10.1002/hipo.1045

Boekhoorn, K., Joels, M., & Lucassen, P. J. (2006). Increased proliferation reflects glial and vascular-associated changes, but not neurogenesis in the presenile Alzheimer hippocampus. *Neurobiology of Disease*, *24*(1), 1–14. https://doi.org/10.1016/j.nbd.2006.04.017

Boldrini, M., Fulmore, C. A., Tartt, A. N., Simeon, L. R., Pavlova, I., Poposka, V., Rosoklija, G. B., Stankov, A., Arango, V., Dwork, A. J., Hen, R., & Mann, J. J. (2018). Human hippocampal neurogenesis persists throughout aging. *Cell Stem Cell*, *22*(4), 589–599 e585. https://doi.org/10.1016/j.stem.2018.03.015

Boldrini, M., Hen, R., Underwood, M. D., Rosoklija, G. B., Dwork, A. J., Mann, J. J., & Arango, V. (2012). Hippocampal angiogenesis and progenitor cell proliferation are increased with antidepressant use in major depression. *Biological Psychiatry*, *72*(7), 562–571. https://doi.org/10.1016/j.biopsych.2012.04.024

Boldrini, M., Underwood, M. D., Hen, R., Rosoklija, G. B., Dwork, A. J., John Mann, J., & Arango, V. (2009). Antidepressants increase neural progenitor cells in the human hippocampus. *Neuropsychopharmacology*, *34*(11), 2376–2389. https://doi.org/10.1038/npp.2009.75

Bottes, S., Jaeger, B. N., Pilz, G. A., Jorg, D. J., Cole, J. D., Kruse, M., Harris, L., Korobeynyk, V. I., Mallona, I., Helmchen, F., Guillemot, F., Simons, B. D., & Jessberger, S. (2021). Long-term self-renewing stem cells in the adult mouse hippocampus identified by intravital imaging. *Nature Neuroscience*, *24*(2), 225–233. https://doi.org/10.1038/s41593-020-00759-4

Bowers, D. C., Gargan, L., Kapur, P., Reisch, J. S., Mulne, A. F., Shapiro, K. N., Elterman, R. D., Winick, N. J., & Margraf, L. R. (2003). Study of the MIB-1 labeling index as a predictor of tumor progression in pilocytic astrocytomas in children and adolescents. *Journal of Clinical Oncology*, *21*(15), 2968–2973. https://doi.org/10.1200/JCO.2003.01.017

Brus, M., Meurisse, M., Gheusi, G., Keller, M., Lledo, P. M., & Levy, F. (2013). Dynamics of olfactory and hippocampal neurogenesis in adult sheep. *Journal of Comparative Neurology*, *521*(1), 169–188. https://doi.org/10.1002/cne.23169

Bunk, E. C., Stelzer, S., Hermann, S., Schafers, M., Schlatt, S., & Schwamborn, J. C. (2011). Cellular organization of adult neurogenesis in the common marmoset. *Aging Cell*, *10*(1), 28–38. https://doi.org/10.1111/j.1474-9726.2010.00639.x

Cavegn, N., van Dijk, R. M., Menges, D., Brettschneider, H., Phalanndwa, M., Chimimba, C. T., Isler, K., Lipp, H. P., Slomianka, L., & Amrein, I. (2013). Habitat-specific shaping of proliferation and neuronal differentiation in adult hippocampal neurogenesis of wild rodents. *Frontiers in Neuroscience*, *7*, 59. https://doi.org/10.3389/fnins.2013.00059

Chawana, R., Alagaili, A., Patzke, N., Spocter, M. A., Mohammed, O. B., Kaswera, C., Gilissen, E., Bennett, N. C., Ihunwo, A. O., & Manger, P. R. (2014). Microbats appear to have adult hippocampal neurogenesis, but post-capture stress causes a rapid decline in the number of neurons expressing doublecortin. *Neuroscience*, *277*, 724–733. https://doi.org/10.1016/j.neuroscience.2014.07.063

Chawana, R., Patzke, N., Alagaili, A. N., Bennett, N. C., Mohammed, O. B., Kaswera-Kyamakya, C., Gilissen, E., Ihunwo, A. O., Pettigrew, J. D., & Manger, P. R. (2016). The distribution of Ki-67 and doublecortin immunopositive cells in the brains of three microchiropteran species, *Hipposideros fuliginosus*, *Triaenops persicus*, and *Asellia tridens*. *Anatomical Record*, *299*(11), 1548–1560. https://doi.org/10.1002/ar.23460

Chawana, R., Patzke, N., Bhagwandin, A., Kaswera-Kyamakya, C., Gilissen, E., Bertelsen, M. F., Hemingway, J., & Manger, P. R. (2020). Adult hippocampal neurogenesis in Egyptian fruit bats from three different environments: Are interpretational variations due to the environment or methodology? *Journal of Comparative Neurology*, *528*(17), 2994–3007. https://doi.org/10.1002/cne.24895

Chawana, R., Patzke, N., Kaswera, C., Gilissen, E., Ihunwo, A. O., & Manger, P. R. (2013). Adult neurogenesis in eight Megachiropteran species. *Neuroscience*, *244*, 159–172. https://doi.org/10.1016/j.neuroscience.2013.04.020

Cipriani, S., Ferrer, I., Aronica, E., Kovacs, G. G., Verney, C., Nardelli, J., Khung, S., Delezoide, A. L., Milenkovic, I., Rasika, S., Manivet, P., Benifla, J. L., Deriot, N., Gressens, P., & Adle-Biassette, H. (2018). Hippocampal radial glial subtypes and their neurogenic potential in human fetuses and healthy and Alzheimer's disease adults. *Cerebral Cortex*, *28*(7), 2458–2478. https://doi.org/10.1093/cercor/bhy096

Clancy, B., & Cauller, L. J. (1998). Reduction of background autofluorescence in brain sections following immersion in sodium borohydride. *Journal of Neuroscience Methods*, *83*(2), 97–102. https://doi.org/10.1016/s0165-0270(98)00066-1

Crews, L., Adame, A., Patrick, C., Delaney, A., Pham, E., Rockenstein, E., Hansen, L., & Masliah, E. (2010). Increased BMP6 levels in the brains of Alzheimer's disease patients and APP transgenic mice are accompanied by impaired neurogenesis. *The Journal of Neuroscience*, *30*(37), 12252–12262. https://doi.org/10.1523/JNEUROSCI.1305-10.2010

D'Alessio, L., Konopka, H., Escobar, E., Acuna, A., Oddo, S., Solis, P., Seoane, E., & Kochen, S. (2015). Dentate gyrus expression of nestin-immunoreactivity in patients with drug-resistant temporal lobe epilepsy and hippocampal sclerosis. *Seizure*, *27*, 75–79. https://doi.org/10.1016/j.seizure.2015.02.008

D'Alessio, L., Konopka, H., Lopez, E. M., Seoane, E., Consalvo, D., Oddo, S., Kochen, S., & Lopez-Costa, J. J. (2010). Doublecortin (DCX) immunoreactivity in hippocampus of chronic refractory temporal lobe epilepsy patients with hippocampal sclerosis. *Seizure*, *19*(9), 567–572. https://doi.org/10.1016/j.seizure.2010.09.004

Dawirs, R. R., Hildebrandt, K., & Teuchert-Noodt, G. (1998). Adult treatment with haloperidol increases dentate granule cell proliferation in the gerbil hippocampus. *Journal of Neural Transmission (Vienna)*, *105*(2–3), 317–327. https://doi.org/10.1007/s007020050061

Dawirs, R. R., Teuchert-Noodt, G., Hildebrandt, K., & Fei, F. (2000). Granule cell proliferation and axon terminal degradation in the dentate gyrus of gerbils (*Meriones unguiculatus*) during maturation, adulthood and aging. *Journal of Neural Transmission (Vienna)*, *107*(6), 639–647. https://doi.org/10.1007/s007020070066

De Nevi, E., Marco-Salazar, P., Fondevila, D., Blasco, E., Perez, L., & Pumarola, M. (2013). Immunohistochemical study of doublecortin and nucleostemin in canine brain. *European Journal of Histochemistry*, *57*(1), e9. https://doi.org/10.4081/ejh.2013.e9

de Ruiter, J. P. (1983). The influence of post-mortem fixation delay on the reliability of the Golgi silver impregnation. *Brain Research*, *266*(1), 143–147. https://doi.org/10.1016/0006-8993(83)91317-3

Del Castillo, P., Llorente, A. R., & Stockert, J. C. (1989). Influence of fixation, exciting light and section thickness on the primary fluorescence of samples for microfluorometric analysis. *Basic and Applied Histochemistry*, *33*(3), 251–257.

Dennis, C. V., Suh, L. S., Rodriguez, M. L., Kril, J. J., & Sutherland, G. T. (2016). Human adult neurogenesis across the ages: An immunohistochemical study. *Neuropathology and Applied Neurobiology*, *42*(7), 621–638. https://doi.org/10.1111/nan.12337

Ding, J., Adiconis, X., Simmons, S. K., Kowalczyk, M. S., Hession, C. C., Marjanovic, N. D., Hughes, T. K., Wadsworth, M. H., Burks, T., Nguyen, L. T., Kwon, J. Y. H., Barak, B., Ge, W., Kedaigle, A. J., Carroll, S., Li, S., Hacohen, N., Rozenblatt-Rosen, O., Shalek, A. K., … Levin, J. Z. (2020). Systematic comparison of single-cell and single-nucleus RNA-sequencing methods. *Nature Biotechnology*, *38*(6), 737–746. https://doi.org/10.1038/s41587-020-0465-8

Du Preez, A., Lefevre-Arbogast, S., Gonzalez-Dominguez, R., Houghton, V., de Lucia, C., Low, D. Y., Helmer, C., Feart, C., Delcourt, C., Proust-Lima, C., Pallas, M., Sanchez-Pla, A., Urpi-Sarda, M., Ruigrok, S. R., Altendorfer, B., Aigner, L., Lucassen, P. J., Korosi, A., Manach, C., … Thuret, S. (2022a). Impaired hippocampal neurogenesis in vitro is modulated by dietary-related endogenous factors and associated with depression in a longitudinal ageing cohort study. *Molecular Psychiatry*. https://doi.org/10.1038/s41380-022-01644-1

Du Preez, A., Lefevre-Arbogast, S., Houghton, V., de Lucia, C., Low, D. Y., Helmer, C., Feart, C., Delcourt, C., Proust-Lima, C., Pallas, M., Ruigrok, S. R., Altendorfer, B., Gonzalez-Dominguez, R., Sanchez-Pla, A., Urpi-Sarda, M., Andres-Lacueva, C., Aigner, L., Lucassen, P. J., Korosi, A., … Thuret, S. (2022b). The serum metabolome mediates the concert of diet, exercise, and neurogenesis, determining the risk for cognitive decline and dementia. *Alzheimer's & Dementia*, *18*(4), 654–675. https://doi.org/10.1002/alz.12428

Ekonomou, A., Savva, G. M., Brayne, C., Forster, G., Francis, P. T., Johnson, M., Perry, E. K., Attems, J., Somani, A., Minger, S. L., & Ballarda, C. G., The Medical Research Council Cognitive Function and Ageing Neuropathology Study. (2015). Stage-specific changes in neurogenic and glial markers in Alzheimer's disease. *Biological Psychiatry*, *77*(8), 711–719. https://doi.org/10.1016/j.biopsych.2014.05.021

Epp, J. R., Barker, J. M., & Galea, L. A. (2009). Running wild: Neurogenesis in the hippocampus across the lifespan in wild and laboratory-bred Norway rats. *Hippocampus*, *19*(10), 1040–1049. https://doi.org/10.1002/hipo.20546

Epp, J. R., Beasley, C. L., & Galea, L. A. (2013). Increased hippocampal neurogenesis and p21 expression in depression: Dependent on antidepressants, sex, age, and antipsychotic exposure. *Neuropsychopharmacology*, *38*(11), 2297–2306. https://doi.org/10.1038/npp.2013.132

Eriksson, P. S., Perfilieva, E., Bjork-Eriksson, T., Alborn, A. M., Nordborg, C., Peterson, D. A., & Gage, F. H. (1998). Neurogenesis in the adult human hippocampus. *Nature Medicine*, *4*(11), 1313–1317. https://doi.org/10.1038/3305

Ernst, A., Alkass, K., Bernard, S., Salehpour, M., Perl, S., Tisdale, J., Possnert, G., Druid, H., & Frisen, J. (2014). Neurogenesis in the striatum of the adult human brain. *Cell*, *156*(5), 1072–1083. https://doi.org/10.1016/j.cell.2014.01.044

Eymin, C., Jordan, D., Saint-Pierre, G., & Kopp, N. (1993). Brain banking for immunocytochemistry and autoradiography. *Journal of Neural Transmission. Supplementum*, *39*, 127–134.

Fasemore, T. M., Patzke, N., Kaswera-Kyamakya, C., Gilissen, E., Manger, P. R., & Ihunwo, A. O. (2018). The distribution of Ki-67 and doublecortin-immunopositive cells in the brains of three strepsirrhine primates: *Galago demidoff*, *Perodicticus potto*, and *Lemur catta*. *Neuroscience*, *372*, 46–57. https://doi.org/10.1016/j.neuroscience.2017.12.037

Flor-Garcia, M., Terreros-Roncal, J., Moreno-Jimenez, E. P., Avila, J., Rabano, A., & Llorens-Martin, M. (2020). Unraveling human adult hippocampal neurogenesis. *Nature Protocols*, *15*(2), 668–693. https://doi.org/10.1038/s41596-019-0267-y

Fowler, C. D., Liu, Y., Ouimet, C., & Wang, Z. (2002). The effects of social environment on adult neurogenesis in the female prairie vole. *Journal of Neurobiology*, *51*(2), 115–128. https://doi.org/10.1002/neu.10042

Franjic, D., Skarica, M., Ma, S., Arellano, J. I., Tebbenkamp, A. T. N., Choi, J., Xu, C., Li, Q., Morozov, Y. M., Andrijevic, D., Vrselja, Z., Spajic, A., Santpere, G., Li, M., Zhang, S., Liu, Y., Spurrier, J., Zhang, L., Gudelj, I., … Sestan, N. (2022). Transcriptomic taxonomy and neurogenic trajectories of adult human, macaque, and pig hippocampal and entorhinal cells. *Neuron*, *110*(3), 452–469 e414. https://doi.org/10.1016/j.neuron.2021.10.036

Galan, L., Gomez-Pinedo, U., Guerrero, A., Garcia-Verdugo, J. M., & Matias-Guiu, J. (2017). Amyotrophic lateral sclerosis modifies progenitor neural proliferation in adult classic neurogenic brain niches. *BMC Neurology*, *17*(1), 173. https://doi.org/10.1186/s12883-017-0956-5

Galea, L. A., & McEwen, B. S. (1999). Sex and seasonal differences in the rate of cell proliferation in the dentate gyrus of adult wild meadow voles. *Neuroscience*, *89*(3), 955–964. https://doi.org/10.1016/s0306-4522(98)00345-5

Gatome, C. W., Mwangi, D. K., Lipp, H. P., & Amrein, I. (2010). Hippocampal neurogenesis and cortical cellular plasticity in Wahlberg's epauletted fruit bat: A qualitative and quantitative study. *Brain, Behavior and Evolution*, *76*(2), 116–127. https://doi.org/10.1159/000320210

Gatt, A., Ekonomou, A., Somani, A., Thuret, S., Howlett, D., Corbett, A., Johnson, M., Perry, E., Attems, J., Francis, P., Aarsland, D., & Ballard, C. (2017). Importance of proactive treatment of depression in Lewy body dementias: The impact on hippocampal neurogenesis and cognition in a post-mortem study. *Dementia and Geriatric Cognitive Disorders*, *44*(5–6), 283–293. https://doi.org/10.1159/000484437

Geha, S., Pallud, J., Junier, M. P., Devaux, B., Leonard, N., Chassoux, F., Chneiweiss, H., Daumas-Duport, C., & Varlet, P. (2010). NG2+/Olig2+ cells are the major cycle-related cell population of the adult human normal brain. *Brain Pathology*, *20*(2), 399–411. https://doi.org/10.1111/j.1750-3639.2009.00295.x

Glees, P., & Hasan, M. (1976). Lipofuscin in neuronal aging and diseases. *Normale und pathologische Anatomie*, *32*, 1–68.

Gomez-Nicola, D., Suzzi, S., Vargas-Caballero, M., Fransen, N. L., Al-Malki, H., Cebrian-Silla, A., Garcia-Verdugo, J. M., Riecken, C., Fehse, C., & Perry, V. H. (2014). Temporal dynamics of hippocampal neurogenesis in chronic neurodegeneration. *Brain*, *137*(Pt 8), 2312–2328. https://doi.org/10.1093/brain/awu155

Gomez-Pinedo, U., Galan, L., Matias-Guiu, J. A., Pytel, V., Moreno, T., Guerrero-Sola, A., & Matias-Guiu, J. (2019). Notch signalling in the hippocampus of patients with motor neuron disease. *Frontiers in Neuroscience*, *13*, 302. https://doi.org/10.3389/fnins.2019.00302

Gould, E., McEwen, B. S., Tanapat, P., Galea, L. A., & Fuchs, E. (1997). Neurogenesis in the dentate gyrus of the adult tree shrew is regulated by psychosocial stress and NMDA receptor activation. *The Journal of Neuroscience*, *17*(7), 2492–2498.

Gould, E., Reeves, A. J., Fallah, M., Tanapat, P., Gross, C. G., & Fuchs, E. (1999). Hippocampal neurogenesis in adult Old World primates. *Proceedings of the National Academy of Sciences of the United States of America*, *96*(9), 5263–5267. https://doi.org/10.1073/pnas.96.9.5263

Gould, E., Tanapat, P., McEwen, B. S., Flugge, G., & Fuchs, E. (1998). Proliferation of granule cell precursors in the dentate gyrus of adult monkeys is diminished by stress. *Proceedings of the National Academy of Sciences of the United States of America*, *95*(6), 3168–3171. https://doi.org/10.1073/pnas.95.6.3168

Goyal, V. K. (1982). Lipofuscin pigment accumulation in human brain during aging. *Experimental Gerontology*, *17*(6), 481–487. https://doi.org/10.1016/s0531-5565(82)80010-7

Grabiec, M., Turlejski, K., & Djavadian, R. L. (2009). The partial 5-HT1A receptor agonist buspirone enhances neurogenesis in the opossum (*Monodelphis domestica*). *European Neuropsychopharmacology*, *19*(6), 431–439. https://doi.org/10.1016/j.euroneuro.2009.01.013

Habib, N., Avraham-Davidi, I., Basu, A., Burks, T., Shekhar, K., Hofree, M., Choudhury, S. R., Aguet, F., Gelfand, E., Ardlie, K., Weitz, D. A., Rozenblatt-Rosen, O., Zhang, F., & Regev, A. (2017). Massively parallel single-nucleus RNA-seq with DroNc-seq. *Nature Methods*, *14*(10), 955–958. https://doi.org/10.1038/nmeth.4407

Hao, Z. Z., Wei, J. R., Xiao, D., Liu, R., Xu, N., Tang, L., Huang, M., Shen, Y., Xing, C., Huang, W., Liu, X., Xiang, M., Liu, Y., Miao, Z., & Liu, S. (2022). Single-cell transcriptomics of adult macaque hippocampus reveals neural precursor cell populations. *Nature Neuroscience*. https://doi.org/10.1038/s41593-022-01073-x

Harman, A., Meyer, P., & Ahmat, A. (2003). Neurogenesis in the hippocampus of an adult marsupial. *Brain, Behavior and Evolution*, *62*(1), 1–12. https://doi.org/10.1159/000071955

Harris, L., Rigo, P., Stiehl, T., Gaber, Z. B., Austin, S. H. L., Masdeu, M. D. M., Edwards, A., Urban, N., Marciniak-Czochra, A., & Guillemot, F. (2021). Coordinated changes in cellular behavior ensure the lifelong maintenance of the hippocampal stem cell population. *Cell Stem Cell*, *28*(5), 863–876 e866. https://doi.org/10.1016/j.stem.2021.01.003

Hauser, T., Klaus, F., Lipp, H. P., & Amrein, I. (2009). No effect of running and laboratory housing on adult hippocampal neurogenesis in wild caught long-tailed wood mouse. *BMC Neuroscience*, *10*, 43. https://doi.org/10.1186/1471-2202-10-43

Hill, A. S., Sahay, A., & Hen, R. (2015). Increasing adult hippocampal neurogenesis is sufficient to reduce anxiety and depression-like behaviors. *Neuropsychopharmacology*, *40*(10), 2368–2378. https://doi.org/10.1038/npp.2015.85

Hochgerner, H., Zeisel, A., Lonnerberg, P., & Linnarsson, S. (2018). Conserved properties of dentate gyrus neurogenesis across postnatal development revealed by single-cell RNA sequencing. *Nature Neuroscience*, *21*(2), 290–299. https://doi.org/10.1038/s41593-017-0056-2

Hoglinger, G. U., Rizk, P., Muriel, M. P., Duyckaerts, C., Oertel, W. H., Caille, I., & Hirsch, E. C. (2004). Dopamine depletion impairs precursor cell proliferation in Parkinson disease. *Nature Neuroscience*, *7*(7), 726–735. https://doi.org/10.1038/nn1265

Hong, X. P., Peng, C. X., Wei, W., Tian, Q., Liu, Y. H., Yao, X. Q., Zhang, Y., Cao, F-Y., Wang, Q., & Wang, J. Z. (2010). Essential role of tau phosphorylation in adult hippocampal neurogenesis. *Hippocampus*, *20*(12), 1339–1349. https://doi.org/10.1002/hipo.20712

Huang, S., Slomianka, L., Farmer, A. J., Kharlamova, A. V., Gulevich, R. G., Herbeck, Y. E., Trut, L. N., & Wolfer, D. P. Amrein, I. (2015). Selection for tameness, a key behavioral trait of domestication, increases adult hippocampal neurogenesis in foxes. *Hippocampus*, *25*(8), 963–975. https://doi.org/10.1002/hipo.22420

Hwang, I. K., Yoo, K. Y., Li, H., Choi, J. H., Kwon, Y. G., Ahn, Y., Lee, IN., & Won, M. H. (2007). Differences in doublecortin immunoreactivity and protein levels in the hippocampal dentate gyrus between adult and aged dogs. *Neurochemical Research*, *32*(9), 1604–1609. https://doi.org/10.1007/s11064-007-9366-1

Islam, A. T., Kuraoka, A., & Kawabuchi, M. (2003). Morphological basis of nitric oxide production and its correlation with the polysialylated precursor cells in the dentate gyrus of the adult Guinea pig hippocampus. *Anatomical Science International*, *78*(2), 98–103. https://doi.org/10.1046/j.0022-7722.2003.00045.x

Jin, K., Peel, A. L., Mao, X. O., Xie, L., Cottrell, B. A., Henshall, D. C., & Greenberg, D. A. (2004). Increased hippocampal neurogenesis in Alzheimer's disease. *Proceedings of the National Academy of Sciences of the United States of America*, *101*(1), 343–347. https://doi.org/10.1073/pnas.2634794100

Johnson, K. M., Boonstra, R., & Wojtowicz, J. M. (2010). Hippocampal neurogenesis in food-storing red squirrels: The impact of age and spatial behavior. *Genes, Brain, and Behavior*, *9*(6), 583–591. https://doi.org/10.1111/j.1601-183X.2010.00589.x

Johnson, M., Ekonomou, A., Hobbs, C., Ballard, C. G., Perry, R. H., & Perry, E. K. (2011). Neurogenic marker abnormalities in the hippocampus in dementia with Lewy bodies. *Hippocampus*, *21*(10), 1126–1136. https://doi.org/10.1002/hipo.20826

Kajimura, J., Ito, R., Manley, N. R., & Hale, L. P. (2016). Optimization of single- and dual-color immunofluorescence protocols for formalin-fixed, paraffin-embedded archival tissues. *Journal of Histochemistry and Cytochemistry*, *64*(2), 112–124. https://doi.org/10.1369/0022155415610792

Kalinina, A., & Lagace, D. (2022). Single-cell and single-nucleus RNAseq analysis of adult neurogenesis. *Cell*, *11*(10), 1633. https://doi.org/10.3390/cells11101633

Kandel, P., Semerci, F., Mishra, R., Choi, W., Bajic, A., Baluya, D., Ma, L., Chen, K., Cao, A. C., Phongmekhin, T., Matinyan, N., Jimenez-Panizo, A., Chamakuri, S., Raji, I. O., Chang, L., Fuentes-Prior, P., MacKenzie, K. R., Benn, C. L., Estebanez-Perpina, E., … Maletic-Savatic, M. (2022). Oleic acid is an endogenous ligand of TLX/NR2E1 that triggers hippocampal neurogenesis. *Proceedings of the National Academy of Sciences of the United States of America*, *119*(13), e2023784119. https://doi.org/10.1073/pnas.2023784119

Kaplan, M. S., & Bell, D. H. (1984). Mitotic neuroblasts in the 9-day-old and 11-month-old rodent hippocampus. *The Journal of Neuroscience*, *4*(6), 1429–1441. https://doi.org/10.1523/JNEUROSCI.04-06-01429.1984

Kempermann, G., Gage, F. H., Aigner, L., Song, H., Curtis, M. A., Thuret, S., Kuhn, H. G., Jessberger, S., Frankland, P. W., Cameron, H. A., Gould, E., Hen, R., Abrous, D. N., Toni, N., Schinder, A. F., Zhao, X., Lucassen, P. J., & Frisen, J. (2018). Human adult neurogenesis: Evidence and remaining questions. *Cell Stem Cell*, *23*(1), 25–30. https://doi.org/10.1016/j.stem.2018.04.004

Kempermann, G., Jessberger, S., Steiner, B., & Kronenberg, G. (2004). Milestones of neuronal development in the adult hippocampus. *Trends in Neurosciences*, *27*(8), 447–452. https://doi.org/10.1016/j.tins.2004.05.013

Knoth, R., Singec, I., Ditter, M., Pantazis, G., Capetian, P., Meyer, R. P., Horvat, V., Volk, B., & Kempermann, G. (2010). Murine features of neurogenesis in the human hippocampus across the lifespan from 0 to 100 years. *PLoS One*, *5*(1), e8809. https://doi.org/10.1371/journal.pone.0008809

Kohler, S. J., Williams, N. I., Stanton, G. B., Cameron, J. L., & Greenough, W. T. (2011). Maturation time of new granule cells in the dentate gyrus of adult macaque monkeys exceeds six months. *Proceedings of the National Academy of Sciences of the United States of America*, *108*(25), 10326–10331. https://doi.org/10.1073/pnas.1017099108

Kornack, D. R., & Rakic, P. (1999). Continuation of neurogenesis in the hippocampus of the adult macaque monkey. *Proceedings of the National Academy of Sciences of the United States of America*, *96*(10), 5768–5773. https://doi.org/10.1073/pnas.96.10.5768

Kumazawa-Manita, N., Hama, H., Miyawaki, A., & Iriki, A. (2013). Tool use specific adult neurogenesis and synaptogenesis in rodent (*Octodon degus*) hippocampus. *PLoS One*, *8*(3), e58649. https://doi.org/10.1371/journal.pone.0058649

Lavenex, P., Steele, M. A., & Jacobs, L. F. (2000). The seasonal pattern of cell proliferation and neuron number in the dentate gyrus of wild adult eastern grey squirrels. *The European Journal of Neuroscience*, *12*(2), 643–648. https://doi.org/10.1046/j.1460-9568.2000.00949.x

Le Maitre, T. W., Dhanabalan, G., Bogdanovic, N., Alkass, K., & Druid, H. (2018). Effects of alcohol abuse on proliferating cells, stem/progenitor cells, and immature neurons in the adult human hippocampus. *Neuropsychopharmacology*, *43*(4), 690–699. https://doi.org/10.1038/npp.2017.251

Leuner, B., Kozorovitskiy, Y., Gross, C. G., & Gould, E. (2007). Diminished adult neurogenesis in the marmoset brain precedes old age. *Proceedings of the National Academy of Sciences of the United States*

of America, *104*(43), 17169–17173. https://doi.org/10.1073/pnas.0708228104

Levy, F., Batailler, M., Meurisse, M., Keller, M., Cornilleau, F., Moussu, C., Poissenot, M. K., & Migaud, M. (2019). Differential effects of oxytocin on olfactory, hippocampal and hypothalamic neurogenesis in adult sheep. *Neuroscience Letters*, *713*, 134520. https://doi.org/10.1016/j.neulet.2019.134520

Li, B., Yamamori, H., Tatebayashi, Y., Shafit-Zagardo, B., Tanimukai, H., Chen, S., Iqbal, K., & Grundke-Iqbal, I. (2008). Failure of neuronal maturation in Alzheimer disease dentate gyrus. *Journal of Neuropathology and Experimental Neurology*, *67*(1), 78–84. https://doi.org/10.1097/nen.0b013e318160c5db

Liu, J., Reeves, C., Jacques, T., McEvoy, A., Miserocchi, A., Thompson, P., Sisodiya, S., & Thom, M. (2018). Nestin-expressing cell types in the temporal lobe and hippocampus: Morphology, differentiation, and proliferative capacity. *Glia*, *66*(1), 62–77. https://doi.org/10.1002/glia.23211

Liu, R. X., Ma, J., Wang, B., Tian, T., Guo, N., & Liu, S. J. (2020). No DCX-positive neurogenesis in the cerebral cortex of the adult primate. *Neural Regeneration Research*, *15*(7), 1290–1299. https://doi.org/10.4103/1673-5374.272610

Liu, Y. W., Curtis, M. A., Gibbons, H. M., Mee, E. W., Bergin, P. S., Teoh, H. H., Connor, B., Dragunow, M., & Faull, R. L. (2008). Doublecortin expression in the normal and epileptic adult human brain. *The European Journal of Neuroscience*, *28*(11), 2254–2265. https://doi.org/10.1111/j.1460-9568.2008.06518.x

Llorens-Martin, M., Torres-Aleman, I., & Trejo, J. L. (2006). Pronounced individual variation in the response to the stimulatory action of exercise on immature hippocampal neurons. *Hippocampus*, *16*(5), 480–490. https://doi.org/10.1002/hipo.20175

Low, V. F., Dragunow, M., Tippett, L. J., Faull, R. L., & Curtis, M. A. (2011). No change in progenitor cell proliferation in the hippocampus in Huntington's disease. *Neuroscience*, *199*, 577–588. https://doi.org/10.1016/j.neuroscience.2011.09.010

Lowe, M. T., Faull, R. L., Christie, D. L., & Waldvogel, H. J. (2015). Distribution of the creatine transporter throughout the human brain reveals a spectrum of creatine transporter immunoreactivity. *The Journal of Comparative Neurology*, *523*(5), 699–725. https://doi.org/10.1002/cne.23667

Lucassen, P. J., Fitzsimons, C. P., Salta, E., & Maletic-Savatic, M. (2020a). Adult neurogenesis, human after all (again): Classic, optimized, and future approaches. *Behavioural Brain Research*, *381*, 112458. https://doi.org/10.1016/j.bbr.2019.112458

Lucassen, P. J., Stumpel, M. W., Wang, Q., & Aronica, E. (2010). Decreased numbers of progenitor cells but no response to antidepressant drugs in the hippocampus of elderly depressed patients. *Neuropharmacology*, *58*(6), 940–949. https://doi.org/10.1016/j.neuropharm.2010.01.012

Lucassen, P. J., Toni, N., Kempermann, G., Frisen, J., Gage, F. H., & Swaab, D. F. (2020b). Limits to human neurogenesis-really? *Molecular Psychiatry*, *25*(10), 2207–2209. https://doi.org/10.1038/s41380-018-0337-5

Lyons, D. M., Buckmaster, P. S., Lee, A. G., Wu, C., Mitra, R., Duffey, L. M., Buckmaster, C. L., Her, S., Patel, P. D., & Schatzberg, A. F. (2010). Stress coping stimulates hippocampal neurogenesis in adult monkeys. *Proceedings of the National Academy of Sciences of the United States of America*, *107*(33), 14823–14827. https://doi.org/10.1073/pnas.0914568107

Malmkvist, J., Brix, B., Henningsen, K., & Wiborg, O. (2012). Hippocampal neurogenesis increase with stereotypic behavior in mink (*Neovison vison*). *Behavioural Brain Research*, *229*(2), 359–364. https://doi.org/10.1016/j.bbr.2012.01.027

Manganas, L. N., Zhang, X., Li, Y., Hazel, R. D., Smith, S. D., Wagshul, M. E., Henn, F., Benveniste, H., Djuric, P. M., Enikolopov, G., & Maletic-Savatic, M. (2007). Magnetic resonance spectroscopy identifies neural progenitor cells in the live human brain. *Science*, *318*(5852), 980–985. https://doi.org/10.1126/science.1147851

Marlatt, M. W., Philippens, I., Manders, E., Czeh, B., Joels, M., Krugers, H., & Lucassen, P. J. (2011). Distinct structural plasticity in the hippocampus and amygdala of the middle-aged common marmoset (*Callithrix jacchus*). *Experimental Neurology*, *230*(2), 291–301. https://doi.org/10.1016/j.expneurol.2011.05.008

Marsh, S. E., Walker, A. J., Kamath, T., Dissing-Olesen, L., Hammond, T. R., de Soysa, T. Y., Young, A. M. H., Murphy, S., Abdulraouf, A., Nadaf, N., Dufort, C., Walker, A. C., Lucca, L. E., Kozareva, V., Vanderburg, C., Hong, S., Bulstrode, H., Hutchinson, P. J., Gaffney, D. J., … Stevens, B. (2022). Dissection of artifactual and confounding glial signatures by single-cell sequencing of mouse and human brain. *Nature Neuroscience*, *25*(3), 306–316. https://doi.org/10.1038/s41593-022-01022-8

Mathews, K. J., Allen, K. M., Boerrigter, D., Ball, H., Shannon Weickert, C., & Double, K. L. (2017). Evidence for reduced neurogenesis in the aging human hippocampus despite stable stem cell markers. *Aging Cell*, *16*(5), 1195–1199. https://doi.org/10.1111/acel.12641

Mattiesen, W. R. C., Tauber, S. C., Gerber, J., Bunkowski, S., Brück, W., & Nau, R. (2009). Increased neurogenesis after hypoxic–ischemic encephalopathy in humans is age related. *Acta Neuropathologica*, *117*(5), 525–534. https://doi.org/10.1007/s00401-009-0509-0

McDonald, H. Y., & Wojtowicz, J. M. (2005). Dynamics of neurogenesis in the dentate gyrus of adult rats. *Neuroscience Letters*, *385*(1), 70–75. https://doi.org/10.1016/j.neulet.2005.05.022

Monje, M. L., Vogel, H., Masek, M., Ligon, K. L., Fisher, P. G., & Palmer, T. D. (2007). Impaired human hippocampal neurogenesis after treatment for central nervous system malignancies. *Annals of Neurology*, *62*(5), 515–520. https://doi.org/10.1002/ana.21214

Moreno-Jimenez, E. P., Flor-Garcia, M., Terreros-Roncal, J., Rabano, A., Cafini, F., Pallas-Bazarra, N., Avila, J., & Llorens-Martin, M. (2019). Adult hippocampal neurogenesis is abundant in neurologically healthy subjects and drops sharply in patients with Alzheimer's disease. *Nature Medicine*, *25*(4), 554–560. https://doi.org/10.1038/s41591-019-0375-9

Moreno-Jimenez, E. P., Terreros-Roncal, J., Flor-Garcia, M., Rabano, A., & Llorens-Martin, M. (2021). Evidences for adult hippocampal neurogenesis in humans. *The Journal of Neuroscience*, *41*(12), 2541–2553. https://doi.org/10.1523/JNEUROSCI.0675-20.2020

Munakata, S., & Hendricks, J. B. (1993). Effect of fixation time and microwave oven heating time on retrieval of the Ki-67 antigen from paraffin-embedded tissue. *The Journal of Histochemistry and Cytochemistry*, *41*(8), 1241–1246. https://doi.org/10.1177/41.8.8331288

Ngwenya, L. B., Peters, A., & Rosene, D. L. (2006). Maturational sequence of newly generated neurons in the dentate gyrus of the young adult rhesus monkey. *The Journal of Comparative Neurology*, *498*(2), 204–216. https://doi.org/10.1002/cne.21045

Olude, A. M., Olopade, J. O., & Ihunwo, A. O. (2014). Adult neurogenesis in the African giant rat (Cricetomysgambianus, waterhouse). *Metabolic Brain Disease*, *29*(3), 857–866. https://doi.org/10.1007/s11011-014-9512-9

Oreja-Guevara, C., Gomez-Pinedo, U., Garcia-Lopez, J., Sanchez-Sanchez, R., Valverde-Moyano, R., Rabano-Gutierrez, A., Matías-Guiu, J. A., González-Suírez, I., Matías-Guiu, J., & Matias-Guiu, J. (2017). Inhibition of neurogenesis in a case of Marburg variant multiple sclerosis. *Multiple Sclerosis and Related Disorders*, *18*, 71–76. https://doi.org/10.1016/j.msard.2017.09.024

Ormerod, B. K., & Galea, L. A. (2001). Reproductive status influences cell proliferation and cell survival in the dentate gyrus of adult female meadow voles: A possible regulatory role for estradiol. *Neuroscience*, *102*(2), 369–379. https://doi.org/10.1016/s0306-4522(00)00474-7

Patzke, N., Kaswera, C., Gilissen, E., Ihunwo, A. O., & Manger, P. R. (2013). Adult neurogenesis in a giant otter shrew (*Potamogale velox*). *Neuroscience*, *238*, 270–279. https://doi.org/10.1016/j.neuroscience.2013.02.025

Patzke, N., LeRoy, A., Ngubane, N. W., Bennett, N. C., Medger, K., Gravett, N., Kaswera-Kyamakya, C., Gilissen E., Chawana, R., & Manger, P. R. (2014). The distribution of doublecortin-immunopositive

cells in the brains of four afrotherian mammals: The Hottentot golden mole (*Amblysomus hottentotus*), the rock hyrax (*Procavia capensis*), the eastern rock sengi (*Elephantulus myurus*) and the four-toed sengi (*Petrodromus tetradactylus*). *Brain, Behavior and Evolution*, *84*(3), 227–241. https://doi.org/10.1159/000367934

Patzke, N., Olaleye, O., Haagensen, M., Hof, P. R., Ihunwo, A. O., & Manger, P. R. (2014). Organization and chemical neuroanatomy of the African elephant (*Loxodonta africana*) hippocampus. *Brain Structure & Function*, *219*(5), 1587–1601. https://doi.org/10.1007/s00429-013-0587-6

Patzke, N., Spocter, M. A., Karlsson, K. A. E., Bertelsen, M. F., Haagensen, M., Chawana, R., Streicher, S., Kaswera, C., Gilissen, E., Alagaili, A. N., Mohammed, O. B., Reep, R. L., Bennett, N. C., Siegel, J. M., Ihunwo, A. O., & Manger, P. R. (2015). In contrast to many other mammals, cetaceans have relatively small hippocampi that appear to lack adult neurogenesis. *Brain Structure & Function*, *220*(1), 361–383. https://doi.org/10.1007/s00429-013-0660-1

Pekcec, A., Baumgartner, W., Bankstahl, J. P., Stein, V. M., & Potschka, H. (2008). Effect of aging on neurogenesis in the canine brain. *Aging Cell*, *7*(3), 368–374. https://doi.org/10.1111/j.1474-9726.2008.00392.x

Peragine, D. E., Simpson, J. A., Mooney, S. J., Lovern, M. B., & Holmes, M. M. (2014). Social regulation of adult neurogenesis in a eusocial mammal. *Neuroscience*, *268*, 10–20. https://doi.org/10.1016/j.neuroscience.2014.02.044

Perrett, C. W., Marchbanks, R. M., & Whatley, S. A. (1988). Characterisation of messenger RNA extracted post-mortem from the brains of schizophrenic, depressed and control subjects. *Journal of Neurology, Neurosurgery, and Psychiatry*, *51*(3), 325–331. https://doi.org/10.1136/jnnp.51.3.325

Perry, E. K., Johnson, M., Ekonomou, A., Perry, R. H., Ballard, C., & Attems, J. (2012). Neurogenic abnormalities in Alzheimer's disease differ between stages of neurogenesis and are partly related to cholinergic pathology. *Neurobiology of Disease*, *47*(2), 155–162. https://doi.org/10.1016/j.nbd.2012.03.033

Pillay, S., Bhagwandin, A., Bertelsen, M. F., Patzke, N., Engler, G., Engel, A. K., & Manger, P. R. (2021). The hippocampal formation of two carnivore species: The feliform banded mongoose and the caniform domestic ferret. *The Journal of Comparative Neurology*, *529*(1), 8–27. https://doi.org/10.1002/cne.25047

Piumatti, M., Palazzo, O., La Rosa, C., Crociara, P., Parolisi, R., Luzzati, F., Lévy, F., & Bonfanti, L. (2018). Non-newly generated, "immature" neurons in the sheep brain are not restricted to cerebral cortex. *The Journal of Neuroscience*, *38*(4), 826–842. https://doi.org/10.1523/JNEUROSCI.1781-17.2017

Reif, A., Fritzen, S., Finger, M., Strobel, A., Lauer, M., Schmitt, A., & Lesch, K. P. (2006). Neural stem cell proliferation is decreased in schizophrenia, but not in depression. *Molecular Psychiatry*, *11*(5), 514–522. https://doi.org/10.1038/sj.mp.4001791

Ritchie, T., Scully, S. A., de Vellis, J., & Noble, E. P. (1986). Stability of neuronal and glial marker enzymes in post-mortem rat brain. *Neurochemical Research*, *11*(3), 383–392. https://doi.org/10.1007/BF00965012

Robinson, A. C., Palmer, L., Love, S., Hamard, M., Esiri, M., Ansorge, O., Lett, D., Attems, J., Morris, C., Troakes, C., Selvackadunco, S., King, A., Al-Sarraj, S., & Mann, D. M. (2016). Extended post-mortem delay times should not be viewed as a deterrent to the scientific investigation of human brain tissue: A study from the Brains for Dementia Research Network Neuropathology Study Group, UK. *Acta Neuropathologica*, *132*(5), 753–755. https://doi.org/10.1007/s00401-016-1617-2

Roeder, S. S., Burkardt, P., Rost, F., Rode, J., Brusch, L., Coras, R., Englund, E., Hakansson, K., Possnert, G., Salehpour, M., Primetzhofer, D., Csiba, L., Molnar, S., Mehes, G., Tonchev, A. B., Schwab, S., Bergmann, O., & Huttner, H. B. (2022). Evidence for postnatal neurogenesis in the human amygdala. *Communications Biology*, *5*(1), 366. https://doi.org/10.1038/s42003-022-03299-8

Royo, J., Villain, N., Champeval, D., Del Gallo, F., Bertini, G., Aujard, F., & Pifferi, F. (2018). Effects of n-3 polyunsaturated fatty acid supplementation on cognitive functions, electrocortical activity and neurogenesis in a non-human primate, the grey mouse lemur (*Microcebus murinus*). *Behavioural Brain Research*, *347*, 394–407. https://doi.org/10.1016/j.bbr.2018.02.029

Sahay, A., Scobie, K. N., Hill, A. S., O'Carroll, C. M., Kheirbek, M. A., Burghardt, N. S., Fenton, A. A., Dranovsky, A., & Hen, R. (2011). Increasing adult hippocampal neurogenesis is sufficient to improve pattern separation. *Nature*, *472*(7344), 466–470. https://doi.org/10.1038/nature09817

Schut, M. H., Patassini, S., Kim, E. H., Bullock, J., Waldvogel, H. J., Faull, R. L. M., Pepers, B. A., den Dunnen, J. T., van Ommen, G. B., & van Roon-Mom, W. M. C. (2017). Effect of post-mortem delay on N-terminal huntingtin protein fragments in human control and Huntington disease brain lysates. *PLoS One*, *12*(6), e0178556. https://doi.org/10.1371/journal.pone.0178556

Seki, T., Hori, T., Miyata, H., Maehara, M., & Namba, T. (2019). Analysis of proliferating neuronal progenitors and immature neurons in the human hippocampus surgically removed from control and epileptic patients. *Scientific Reports*, *9*(1), 18194. https://doi.org/10.1038/s41598-019-54684-z

Shi, S. R., Imam, S. A., Young, L., Cote, R. J., & Taylor, C. R. (1995). Antigen retrieval immunohistochemistry under the influence of pH using monoclonal antibodies. *The Journal of Histochemistry and Cytochemistry*, *43*(2), 193–201. https://doi.org/10.1177/43.2.7822775

Shors, T. J., Miesegaes, G., Beylin, A., Zhao, M., Rydel, T., & Gould, E. (2001). Neurogenesis in the adult is involved in the formation of trace memories. *Nature*, *410*(6826), 372–376. https://doi.org/10.1038/35066584

Siew, L. K., Love, S., Dawbarn, D., Wilcock, G. K., & Allen, S. J. (2004). Measurement of pre- and post-synaptic proteins in cerebral cortex: Effects of post-mortem delay. *Journal of Neuroscience Methods*, *139*(2), 153–159. https://doi.org/10.1016/j.jneumeth.2004.04.020

Siwak-Tapp, C. T., Head, E., Muggenburg, B. A., Milgram, N. W., & Cotman, C. W. (2007). Neurogenesis decreases with age in the canine hippocampus and correlates with cognitive function. *Neurobiology of Learning and Memory*, *88*(2), 249–259. https://doi.org/10.1016/j.nlm.2007.05.001

Slomianka, L., Drenth, T., Cavegn, N., Menges, D., Lazic, S. E., Phalanndwa, M., Chimimba. C. T., & Amrein, I. (2013). The hippocampus of the eastern rock sengi: Cytoarchitecture, markers of neuronal function, principal cell numbers, and adult neurogenesis. *Frontiers in Neuroanatomy*, *7*, 34. https://doi.org/10.3389/fnana.2013.00034

Smith, T. W., & Lippa, C. F. (1995). Ki-67 immunoreactivity in Alzheimer's disease and other neurodegenerative disorders. *Journal of Neuropathology and Experimental Neurology*, *54*(3), 297–303. https://doi.org/10.1097/00005072-199505000-00002

Sorensen, K. V. (1984). Rapid post-mortem decomposition of the somatostatin cells in human brain. An immunohistochemical examination. *Biomedicine & Pharmacotherapy*, *38*(9-10), 458–461.

Sorrells, S. F., Paredes, M. F., Cebrian-Silla, A., Sandoval, K., Qi, D., Kelley, K. W., James, D., Mayer, S., Chang, J., Auguste, K. I., Chang, E. F., Gutierrez, A. J., Kriegstein, A. R., Mathern, G. W., Oldham, M. C., Huang, E. J., Garcia-Verdugo, J. M., Yang, Z., & Alvarez-Buylla, A. (2018). Human hippocampal neurogenesis drops sharply in children to undetectable levels in adults. *Nature*, *555*(7696), 377–381. https://doi.org/10.1038/nature25975

Sorrells, S. F., Paredes, M. F., Zhang, Z., Kang, G., Pastor-Alonso, O., Biagiotti, S., Page, C. E., Sandoval, K., Knox, A., Connolly, A., Huang, E. J., Garcia-Verdugo, J. M., Oldham, M. C., Yang, Z., & Alvarez-Buylla, A. (2021). Positive controls in adults and children support that very few, if any, new neurons are born in the adult human hippocampus. *The Journal of Neuroscience*, *41*(12), 2554–2565. https://doi.org/10.1523/JNEUROSCI.0676-20.2020

Spalding, K. L., Bergmann, O., Alkass, K., Bernard, S., Salehpour, M., Huttner, H. B., Bostrom, E., Westerlund, I., Vial, C., Buchholz, B. A., Possnert, G., Mash, D. C., Druid, H., & Frisen, J. (2013). Dynamics of hippocampal neurogenesis in adult humans. *Cell*, *153*(6), 1219–1227. https://doi.org/10.1016/j.cell.2013.05.002

Stepien, T., Tarka, S., Chutoranski, D., Felczak, P., Acewicz, A., & Wierzba-Bobrowicz, T. (2018). Neurogenesis in adult human brain after hemorrhage and ischemic stroke. *Folia Neuropathologica*, *56*(4), 293–300. https://doi.org/10.5114/fn.2018.80862

Sun, Y., Ip, P., & Chakrabartty, A. (2017). Simple elimination of background fluorescence in formalin-fixed human brain tissue for immunofluorescence microscopy. *Journal of Visualized Experiments*, (127), 56188. https://doi.org/10.3791/56188

Takamori, Y., Wakabayashi, T., Mori, T., Kosaka, J., & Yamada, H. (2014). Organization and cellular arrangement of two neurogenic regions in the adult ferret (*Mustela putorius furo*) brain. *The Journal of Comparative Neurology*, *522*(8), 1818–1838. https://doi.org/10.1002/cne.23503

Tamura, Y., Takahashi, K., Takata, K., Eguchi, A., Yamato, M., Kume, S., Nakano, M., Watanabe, Y., & Kataoka, Y. (2016). Noninvasive evaluation of cellular proliferative activity in brain neurogenic regions in rats under depression and treatment by enhanced [18F]FLT-PET imaging. *The Journal of Neuroscience*, *36*(31), 8123–8131. https://doi.org/10.1523/JNEUROSCI.0220-16.2016

Tartt, A. N., Fulmore, C. A., Liu, Y., Rosoklija, G. B., Dwork, A. J., Arango, V., Hen, R., Mann, J. J., & Boldrini, M. (2018). Considerations for assessing the extent of hippocampal neurogenesis in the adult and aging human brain. *Cell Stem Cell*, *23*(6), 782–783. https://doi.org/10.1016/j.stem.2018.10.025

Taylor, C. R., Shi, S. R., Chaiwun, B., Young, L., Imam, S. A., & Cote, R. J. (1994). Strategies for improving the immunohistochemical staining of various intranuclear prognostic markers in formalin-paraffin sections: Androgen receptor, estrogen receptor, progesterone receptor, p53 protein, proliferating cell nuclear antigen, and Ki-67 antigen revealed by antigen retrieval techniques. *Human Pathology*, *25*(3), 263–270. https://doi.org/10.1016/0046-8177(94)90198-8

Terreros-Roncal, J., Moreno-Jimenez, E. P., Flor-Garcia, M., Rodriguez-Moreno, C. B., Trinchero, M. F., Cafini, F., Rabano, A., & Llorens-Martin, M. (2021). Impact of neurodegenerative diseases on human adult hippocampal neurogenesis. *Science*, *374*(6571), 1106–1113. https://doi.org/10.1126/science.abl5163

Terreros-Roncal, J., Moreno-Jimenez, E. P., Flor-Garcia, M., Rodriguez-Moreno, C. B., Trinchero, M. F., Marquez-Valadez, B., Cafini, F., Rabano, A., & Llorens-Martin, M. (2022a). Response to comment on "Impact of neurodegenerative diseases on human adult hippocampal neurogenesis". *Science*, *376*(6590), eabn7270. https://doi.org/10.1126/science.abn7270

Terreros-Roncal, J., Moreno-Jimenez, E. P., Flor-Garcia, M., Rodriguez-Moreno, C. B., Trinchero, M. F., Marquez-Valadez, B., Cafini, F., Rabano, A., & Llorens-Martin, M. (2022b). Response to comment on "Impact of neurodegenerative diseases on human adult hippocampal neurogenesis". *Science*, *376*(6590), eabo0920. https://doi.org/10.1126/science.abo0920

Terstege, D. J., Addo-Osafo, K., Campbell Teskey, G., & Epp, J. R. (2022). New neurons in old brains: Implications of age in the analysis of neurogenesis in post-mortem tissue. *Molecular Brain*, *15*(1), 38. https://doi.org/10.1186/s13041-022-00926-7

Tobin, M. K., Musaraca, K., Disouky, A., Shetti, A., Bheri, A., Honer, W. G., Kim, N., Dawe, R. J., Bennett, D. A., Arfanakis, K., & Lazarov, O. (2019). Human hippocampal neurogenesis persists in aged adults and Alzheimer's disease patients. *Cell Stem Cell*, *24*(6), 974–982 e973. https://doi.org/10.1016/j.stem.2019.05.003

Tonchev, A. B., & Yamashima, T. (2006). Differential neurogenic potential of progenitor cells in dentate gyrus and CA1 sector of the postischemic adult monkey hippocampus. *Experimental Neurology*, *198*(1), 101–113. https://doi.org/10.1016/j.expneurol.2005.11.022

Tonchev, A. B., Yamashima, T., Zhao, L., Okano, H. J., & Okano, H. (2003). Proliferation of neural and neuronal progenitors after global brain ischemia in young adult macaque monkeys. *Molecular and Cellular Neurosciences*, *23*(2), 292–301. https://doi.org/10.1016/s1044-7431(03)00058-7

Tran, M. N., Maynard, K. R., Spangler, A., Huuki, L. A., Montgomery, K. D., Sadashivaiah, V., Tippani, M., Barry, B. K., Hancock, D. B., Hicks, S. C., Kleinman, J. E., Hyde, T. M., Collado-Torres, L., Jaffe, A. E., & Martinowich, K. (2021). Single-nucleus transcriptome analysis reveals cell-type-specific molecular signatures across reward circuitry in the human brain. *Neuron*, *109*(19), 3088–3103 e3085. https://doi.org/10.1016/j.neuron.2021.09.001

Verwer, R. W. H., Sluiter, A. A., Balesar, J. C., Noske, D. P., Dirven, C. M. F., Wouda, J., van Dam, A. M., Lucassen, P. J., & Swaab, D. F. (2007). Mature astrocytes in the adult human neocortex express the early neuronal marker doublecortin. *Brain*, *130*(12), 3321–3335. https://doi.org/10.1093/brain/awm264

Wan, L., Huang, R. J., Yang, C., Ai, J. Q., Zhou, Q., Gong, J. E., Li, J., Zhang, Y., Luo, Z-H., Tu, E., Pan, A., Xiao, B., & Yan, X. X. (2021). Extracranial (125)I seed implantation allows non-invasive stereotactic radioablation of hippocampal adult neurogenesis in Guinea pigs. *Frontiers in Neuroscience*, *15*, 756658. https://doi.org/10.3389/fnins.2021.756658

Wan, L., Tu, T., Zhang, Q. L., Jiang, J., & Yan, X. X. (2019). Pregnancy promotes maternal hippocampal neurogenesis in Guinea pigs. *Neural Plasticity*, *2019*, 5765284. https://doi.org/10.1155/2019/5765284

Wang, W., Wang, M., Yang, M., Zeng, B., Qiu, W., Ma, Q., Jing, X., Zhang, Q., Wang, B., Yin, C., Zhang, J., Ge, Y., Lu, Y., Ji, W., Wu, Q., Ma, C., & Wang, X. (2022). Transcriptome dynamics of hippocampal neurogenesis in macaques across the lifespan and aged humans. *Cell Research*. https://doi.org/10.1038/s41422-022-00678-y

Wang, Y., TesFaye, E., Yasuda, R. P., Mash, D. C., Armstrong, D. M., & Wolfe, B. B. (2000). Effects of post-mortem delay on subunits of ionotropic glutamate receptors in human brain. *Brain Research. Molecular Brain Research*, *80*(2), 123–131. https://doi.org/10.1016/s0169-328x(00)00111-x

Willingham, M. C. (1983). An alternative fixation-processing method for preembedding ultrastructural immunocytochemistry of cytoplasmic antigens: The GBS (glutaraldehyde-borohydride-saponin) procedure. *The Journal of Histochemistry and Cytochemistry*, *31*(6), 791–798. https://doi.org/10.1177/31.6.6404984

Winner, B., Regensburger, M., Schreglmann, S., Boyer, L., Prots, I., Rockenstein, E., Mante, M., Zhao, C., Winkler, J., Masliah, E., & Gage, F. H. (2012). Role of alpha-synuclein in adult neurogenesis and neuronal maturation in the dentate gyrus. *The Journal of Neuroscience*, *32*(47), 16906–16916. https://doi.org/10.1523/JNEUROSCI.2723-12.2012

Zhao, C., Teng, E. M., Summers, R. G., Jr., Ming, G. L., & Gage, F. H. (2006). Distinct morphological stages of dentate granule neuron maturation in the adult mouse hippocampus. *Journal of Neuroscience*, *26*(1), 3–11. https://doi.org/10.1523/JNEUROSCI.3648-05.2006

Zhou, Y., Su, Y., Li, S., Kennedy, B. C., Zhang, D. Y., Bond, A. M., Sun, Y., Jacob, F., Lu, L., Hu, P., Viaene, A. N., Helbig, I., Kessler, S. K., Lucas, T., Salinas, R. D., Gu, X., Chen, H. I., Wu, H., Kleinman, J. E., … Song, H. (2022). Molecular landscapes of human hippocampal immature neurons across lifespan. *Nature*. https://doi.org/10.1038/s41586-022-04912-w

Zhu, H., Wang, Z. Y., & Hansson, H. A. (2003). Visualization of proliferating cells in the adult mammalian brain with the aid of ribonucleotide reductase. *Brain Research*, *977*(2), 180–189. https://doi.org/10.1016/s0006-8993(03)02627-1

How to cite this article: Terreros-Roncal, J., Flor-García, M., Moreno-Jiménez, E. P., Rodríguez-Moreno, C. B., Márquez-Valadez, B., Gallardo-Caballero, M., Rábano, A., & Llorens-Martín, M. (2023). Methods to study adult hippocampal neurogenesis in humans and across the phylogeny. *Hippocampus*, *33*(4), 271–306. https://doi.org/10.1002/hipo.23474